ELSEVIER

Biochimica et Biophysica Acta 1554 (2002) 75–93

BIOCHIMICA ET BIOPHYSICA ACTA
BBA

www.bba-direct.com

Tuning of the optical and electrochemical properties of the primary donor bacteriochlorophylls in the reaction centre from *Rhodobacter sphaeroides*: spectroscopy and structure

Diane Spiedel [a], Aleksander W. Roszak [b,c], Kimberley McKendrick [c], Katherine E. McAuley [b,c,1], Paul K. Fyfe [d], Eliane Nabedryk [e], Jacques Breton [e], Bruno Robert [f], Richard J. Cogdell [c], Neil W. Isaacs [b], Michael R. Jones [e,*]

[a] *Department of Molecular Biology and Biotechnology, University of Sheffield, Western Bank, Sheffield, S10 2UH, UK*
[b] *Department of Chemistry, University of Glasgow, Glasgow, G12 8QQ, UK*
[c] *Division of Biochemistry and Molecular Biology, University of Glasgow, Glasgow, G12 8QQ, UK*
[d] *Department of Biochemistry, School of Medical Sciences, University of Bristol, University Walk, Bristol, BS8 1TD, UK*
[e] *Section de Bioénergétique, DBCM/CEA and URA 1290 CNRS, CEA-Saclay, 91191 Gif/Yvette, France*
[f] *Section de Biophysique des Protéines et des Membranes, DBCM/CEA and URA 1290 CNRS, CEA-Saclay, 91191 Gif/Yvette, France*

Received 24 January 2002; received in revised form 25 March 2002; accepted 11 April 2002

Abstract

A series of mutations have been introduced at residue 168 of the L-subunit of the reaction centre from *Rhodobacter sphaeroides*. In the wild-type reaction centre, residue His L168 donates a strong hydrogen bond to the acetyl carbonyl group of one of the pair of bacteriochlorophylls (BChl) that constitutes the primary donor of electrons. Mutation of His L168 to Phe or Leu causes a large decrease in the mid-point redox potential of the primary electron donor, consistent with removal of this strong hydrogen bond. Mutations to Lys, Asp and Arg cause smaller decreases in redox potential, indicative of the presence of weak hydrogen bond and/or an electrostatic effect of the polar residue. A spectroscopic analysis of the mutant complexes suggests that replacement of the wild-type His residue causes a decrease in the strength of the coupling between the two primary donor bacteriochlorophylls. The X-ray crystal structure of the mutant in which His L168 has been replaced by Phe (HL168F) was determined to a resolution of 2.5 Å, and the structural model of the HL168F mutant was compared with that of the wild-type complex. The mutation causes a shift in the position of the primary donor bacteriochlorophyll that is adjacent to residue L168, and also affects the conformation of the acetyl carbonyl group of this bacteriochlorophyll. This conformational change constitutes an approximately 27° through-plane rotation, rather than the large into-plane rotation that has been widely discussed in the context of the HL168F mutation. The possible structural basis of the altered spectroscopic properties of the HL168F mutant reaction centre is discussed, as is the relevance of the X-ray crystal structure of the HL168F mutant to the possible structures of the remaining mutant complexes.

Keywords: Bacteriophyll; *Rhodobacter sphaeroides*; Spectroscopy

1. Introduction

Reaction centres are integral membrane protein complexes that play a central role in the conversion of light energy into a biologically useful form. In the purple bacterium *Rhodobacter* (*Rb.*) *sphaeroides*, the reaction centre consists of three subunits, termed H, L and M, that encase 10 cofactors. These are four molecules of bacteriochlorophyll (BChl), two molecules of bacteriopheophytin (BPhe), two molecules of ubiquinone, a single photoprotective carotenoid and a non-heme iron atom. The X-ray crystal

Abbreviations: BChl, bacteriochlorophyll; BPhe, bacteriopheophytin; Fe, non-heme iron; LDAO, lauryldimethylamine oxide; P, primary donor of electrons; P^+, primary donor cation radical; PMS, phenazine methosulfate; PES, phenazine ethosulfate; TMPD, *N,N,N′,N′* -tetramethyl-1,4,-phenylenediamine; *Rb.*, *Rhodobacter*; *Rps.*, *Rhodopseudomonas*; Spo, spheroidenone; Ubi, ubiquinone

* Corresponding author. Department of Biochemistry, School of Medical Sciences, University of Bristol, University Walk, Bristol, BS8 1TD, UK. Tel.: +44-117-9287571; fax: +44-117-9288274.
E-mail address: m.r.jones@bristol.ac.uk (M.R. Jones).
[1] Present address: Daresbury Laboratories, Daresbury, Warrington, WA4 4AD, UK.

0005-2728/02/$ - see front matter
PII: S0005-2728(02)00215-3

structure of the *Rb. sphaeroides* reaction centre reveals that the BChl, BPhe and ubiquinone cofactors are arranged around an axis of pseudo twofold symmetry in two membrane-spanning branches [1–4]. Spectroscopic studies have shown that the reaction centre catalyses a picosecond timescale, light-driven transmembrane electron transfer that, in turn, initiates a cycle of electron transfer reactions that is coupled to proton translocation across the bacterial cytoplasmic membrane (see Refs. [5–10] for reviews). In the initial steps, light energy drives electron transfer from a pair of excitonically coupled BChl molecules located near the periplasmic side of the membrane, to a molecule of ubiquinone located near the cytoplasmic side of the membrane. This transmembrane electron transfer involves an intervening monomeric BChl (B_L) and a molecule of bacteriopheophytin (BPhe, denoted H_L) [5–10].

An obvious function of the protein component of the reaction centre is to provide a scaffold that holds the various cofactors at fixed distances and relative geometries. Interactions between the cofactors affect their individual optical, electrochemical and electronic properties. In addition to this, the protein environment modulates the biophysical properties of the cofactors through specific protein–cofactor interactions. A good illustration of this is the hydrogen bond donated by the histidine residue at position 168 of the L-subunit (His L168) to the acetyl carbonyl group of one of the BChls of the excitonically coupled pair described above (Fig. 1). The BChl that interacts with residue His L168 is denoted as P_L (where P refers to the primary donor of electrons), whilst the partner BChl is denoted as P_M (Fig. 1). The two BChls are related by the axis of twofold symmetry described above.

In BChl, the acetyl carbonyl group is conjugated to the π electron system of the macrocycle, and so provides an opportunity for the protein to exert significant effects on the biophysical properties of the macrocycle (Fig. 1). The 2a carbon of the carbonyl group is connected by a C–C bond to carbon 2 of ring I of the BChl macrocycle (Fig. 1A). The geometry of the acetyl group relative to the plane of the BChl macrocycle is therefore not fixed, and will depend on degree of rotation around the C2–C2a bond. Furthermore, it is believed that the extent to which the acetyl carbonyl group is conjugated to the rest of the π electron system of the macrocycle is dependent upon the geometry of the group relative to the plane of the macrocycle, decreasing in strength as the carbonyl group is rotated out of the plane of the macrocycle [11].

In the reaction centre, the acetyl carbonyl groups of the P BChls are located close to the region where the P_L and P_M halves of the dimer overlap (Fig. 1B). The acetyl carbonyl of the P_L BChl engages in a hydrogen bond interaction with the side-chain of the adjacent His L168 amino acid (Fig. 1B). The (symmetry-related) acetyl carbonyl of the P_M BChl is not hydrogen bonded, as the symmetry-related residue to His L168 is a phenylalanine (M197). Residue His L168 is conserved in all of the (~ 50) available sequences for the

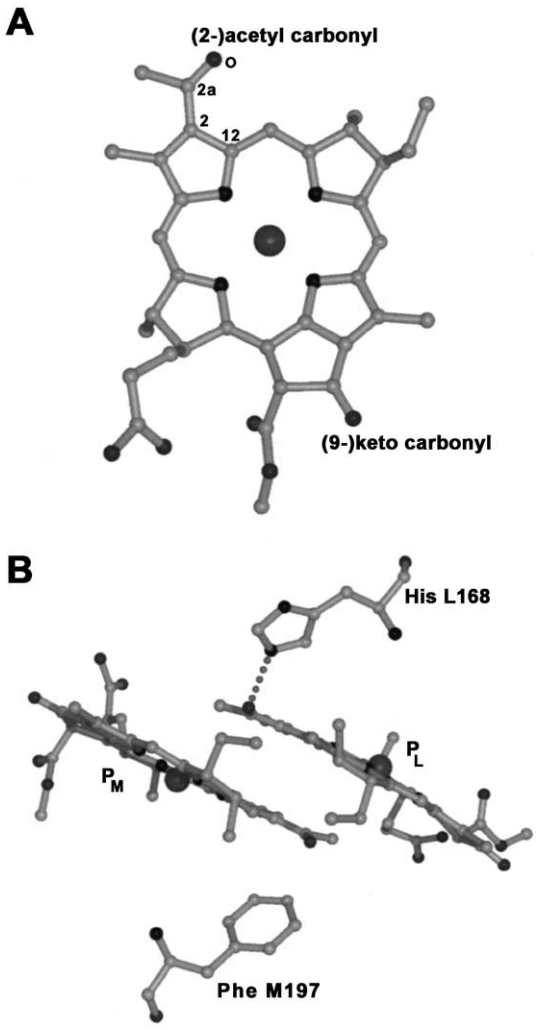

Fig. 1. (A) Bacteriochlorophyll, with the hydrocarbon side-chain omitted, showing the positions of the acetyl and keto carbonyl groups. (B) The primary donor BChls in the wild-type *Rb. sphaeroides* reaction centre, showing the position of residue His L168, the hydrogen bond connection to the acetyl carbonyl of P_L (dotted line), and the symmetry-related residue Phe M197. Key: light grey—carbon; mid grey—oxygen; black—nitrogen, sphere—magnesium.

pufL gene with the exception of six species of *Acidiphilum*, where the equivalent residue is Glu [12].

Extensive studies have shown that mutagenesis of residue His L168 to Phe (HL168F) alters the biophysical properties of the P dimer [13–20]. The mutation abolishes the hydrogen bond interaction between the acetyl carbonyl of the P_L BChl and the L168 residue [17], and this is accompanied by a decrease in the mid-point redox potential of the P/P^+ redox couple (E_m P/P^+) [15,17]. In addition, the HL168F mutation brings about a significant change in the optical properties of the P BChls [14], shifting the absorbance band attributable to the low energy component of the Q_y optical transition of P (P Q_y band) to higher energies by some 15 nm at room temperature [14] and 20 nm at 20 K [19]. The mutation also affects the electronic structure of the cation radical of the P dimer (P^+), causing a

shift in the distribution of spin density between the two BChls of the P dimer [20]. In the wild-type reaction centre, 68% of the positive charge of the cation is located on the P_L half of the dimer, and the proportion decreases to 43% in the HL168F mutant [20].

In this work, we have studied the spectroscopic properties of reaction centres with a number of different mutations at the L168 position. Two of the mutations, to Phe (HL168F) and Leu (HL168L), were made with a view to breaking the hydrogen bond between the P_L BChl and the L168 residue through substitution of the His with apolar residues that are different in terms of size and aromaticity. In addition to conducting a spectroscopic analysis, we have also determined the X-ray crystal structure of the HL168F mutant, to a resolution of 2.5 Å. The remaining mutations, to Asp (HL168D), Lys (HL168K) and Arg (HL168R), were made with a view to testing the ability of acidic or basic residues to act as a hydrogen bond donor. We describe the effects of the different mutations on the spectroscopic properties of the reaction centre cofactors, and discuss the possible structural origins of these effects. Finally, we compare the results of our crystallographic study with the recently reported X-ray crystal structure of a HL168F mutant of the *Rhodopseudomonas* (*Rps.*) *viridis* reaction centre [21].

2. Materials and methods

2.1. Experimental material

Antenna-deficient strains of *Rb. sphaeroides* containing reaction centres with the mutation HL168F, HL168L, HL168D, HL168K and HL168R were constructed as described previously for the HL168F mutant [22]. Cell growth, the preparation of intracytoplasmic membranes and the purification of reaction centres for spectroscopy were carried out as reported elsewhere [23].

Room temperature absorption spectra were recorded using a Beckman DU640 scanning spectrophotometer. Sodium ascorbate and phenazine methosulfate (PMS) were added to final concentrations of 1 mM and 25 μM, respectively, to ensure full reduction of the P BChls. Spectra of chemically oxidized reaction centres were obtained by the addition of potassium ferricyanide to final concentration of up to 50 mM.

Low temperature (30 K) absorption spectra were recorded on a Cary 5 spectrophotometer fitted with a liquid helium cryostat. Intracytoplasmic membranes or purified reaction centres were suspended in 60% glycerol and placed in a plastic cuvette of either 2- or 4-mm path length. The concentration of reaction centres or membranes was adjusted to achieve an OD at 802 nm of approximately 0.2. Where required, sodium ascorbate/PMS or potassium ferricyanide was added to the final concentrations described above for room temperature absorption spectroscopy.

2.2. Redox potentiometry

Values of E_m P/P^+ were determined by chemical titration. Intracytoplasmic membranes were diluted to a reaction centre concentration of approximately 0.6 μM in 100 mM potassium phosphate buffer (pH 7.8) that had been bubbled with oxygen-free nitrogen, and were placed in a home-built glass cuvette that was continuously purged with oxygen-free nitrogen. Redox mediators were added to the following concentrations: PMS, 2 μM; phenazine ethosulfate (PES), 2 μM; and *N,N,N′,N′* -tetramethyl-1,4,-phenylenediamine (TMPD), 10 μM. The ambient redox potential was adjusted by small additions of potassium ferricyanide or sodium ascorbate, and was monitored using a micro combination platinum electrode (Kent ABB). Prior to starting the titration, the electrode was calibrated using a fresh equimolar (10 mM) solution of ferri- and ferrocyanide [24]. The percentage of P in the reduced state was determined by measuring the amplitude of the P Q_y absorbance band relative to that in a sample of fully reduced reaction centres, using a Beckman DU640 scanning spectrophotometer. The amplitude of the band was plotted as function of the redox potential, and the data were fitted with a Nernst curve with $n=1$.

2.3. Fourier transform Raman (FT-Raman) spectroscopy

FT-Raman spectra were recorded at room temperature using a Bruker IFS 66 interferometer coupled to a Bruker FRA 106 Raman module. Excitation was provided at 1064 nm by a diode-pumped Nd/YAG laser operating in a continuous wave mode. Excitation at this wavelength is in pre-resonance with the P Q_y absorbance band, allowing detection of the vibrational modes that would be detected under resonance conditions. Although it might be expected that the blue-shift of the P Q_y band observed in the mutant reaction centres would cause a (small) change in the intensity of the entire FT-Raman spectrum, the relative intensity of individual bands (such as one of the carbonyl bands) will not be affected by such spectral shifts.

Raman photons were collected with a 180° back-scattering geometry with a spectral resolution of 4 cm^{-1}. The sample consisted of purified reaction centres that had been concentrated to an OD at 804 nm of between 60 and 150 units ml^{-1}. Solid sodium ascorbate was added to the reaction centres to prevent oxidation of P. Crystals of potassium ferricyanide were added to obtain spectra of chemically oxidized reaction centres. The samples were placed into a sapphire ball, and this was carefully aligned in the sample holder. Spectra were obtained by the co-addition of 4000–8000 interferograms.

2.4. Fourier transform infrared (FTIR) spectroscopy

Light-induced FTIR difference spectra were recorded using a Nicolet 60 SX FTIR spectrometer equipped with a

MCT-A detector and a KBr beam-splitter. For each reaction centre, intracytoplasmic membranes were dried onto a CaF_2 disk under a flow of N_2. The water content of the samples was controlled by keeping the ratio of absorbance at 1650 and 3300 cm^{-1} between 0.4 and 0.8. The film was sealed in an air tight CaF_2 cuvette and cooled in a temperature controlled cryostat. Light-induced FTIR spectra were obtained under steady-state continuous illumination at 100 K. Cycles of illumination were repeated several hundred times. Spectra were typically the average of 64 000 interferograms, and the resolution was 4 cm^{-1}.

2.5. Crystallization and X-ray crystallography

Purification of the HL168F mutant reaction centre for crystallization was carried out using the detergent lauryldimethylamine oxide (LDAO), as described previously [25]. Crystallization of the HL168F reaction centre was carried out using trisodium citrate as the precipitant, as described in detail elsewhere [26]. Trigonal crystals appeared within 4 weeks and grew as prisms of variable size, ranging from 0.3 to 1 mm in the longest dimension. The crystals belonged to the space group $P3_121$ and had unit cell dimensions of $a=b=141.7$ Å, $c=186.4$ Å, $\alpha=\beta=90°$, $\gamma=120°$.

Diffraction data (27.0–2.50 Å) were collected at the EMBL BW7B beam-line at HASYLAB/DESY, Hamburg, using one crystal at a temperature of 100 K. Cryo-protection of the crystal was achieved by stepwise addition and subsequent removal of aliquots of cryo-protectant solution to the crystal in mother liquor. The cryo-protectant solution was 10% (*R*,*R*)-2,3-butanediol, 3.5% heptane-1,2,3-triol, 1.4 M potassium phosphate, 0.45% LDAO (pH 8.0). The data were collected using a MAR345 image plate and processed with the programs Denzo and Scalepack [27]. The coordinates of the wild-type reaction centre from *Rb. sphaeroides* strain RCO2 [25], with His L168 replaced by Ala, the Q_B ubiquinone removed and all solvent molecules omitted, were used as the starting model for the molecular replacement with AMoRe [28]. The solution from AMoRe (with a correlation coefficient of 80.3% and an R-factor of 29.0%) was subsequently used in a multi-domain rigid-body refinement (each protein chain and cofactor treated as a separate domain) with the program REFMAC [29]. Electron density maps calculated after this stage clearly showed density for a Phe side-chain at the L168 position, and the need for a through-plane rotation of the acetyl group of the P_L BChl. All modeling works, including fitting of the L168 residue, the Q_B ubiquinone-10, a number of LDAO-detergent molecules and all water molecules, were performed using QUANTA (Molecular Simulations Inc.). Restrained maximum likelihood refinement with individual atom isotropic displacement parameters, fixed hydrogen atom contributions and new internal bulk solvent correction was carried out with REFMAC5, using the full set of data collected in the 27.0–2.5 Å resolution range. At this stage, based on the values of individual atomic temperature factors, the occupancy of the Q_B ubiquinone-10 was changed to 0.5. Similarly, the occupancies of individual detergent molecules were changed to a value from the range 0.5–1.0.

Prior to the final isotropic refinement of the structure, TLS parametrisation and the TLS refinement were applied to derive the anisotropic motions (*T*ranslations, *L*ibrations and *S*crew-rotations) of the whole reaction centre complex treated as a pseudo-rigid body [30]. The subsequent and final refinement with isotropic displacement parameters produced improved refinement statistics (R factor lower by 2.6%, and R_{free} lower by 3.2%) and much better estimation of the local internal atomic displacements. Table 2 presents the statistics for the diffraction data and for the final refinement.

Figures were prepared using the programs Molscript [31], Raster3D [32] and XtalView [33].

3. Results

3.1. Mutant construction and absorbance spectroscopy

As described in Materials and methods, five mutations were introduced at the L168 position. The mutated reaction centre genes were expressed in a strain of *Rb. sphaeroides* that lacks the structural genes for the LH1 and LH2 antenna complexes [34], leaving the reaction centre as the sole pigment–protein complex. The control strain containing wild-type reaction centres was strain RCO2 [35].

Room temperature absorbance spectroscopy of bacterial cells and antenna-deficient intracytoplasmic membranes showed that none of the mutations affected the expression level of the reaction centre (data not shown). In the region between 700 and 950 nm, the reaction centre bacteriochlorins give rise to three absorbance bands. The band at 756 nm in membrane-bound reaction centres is attributable to the Q_y transitions of the reaction centre BPhes (H Q_y band). The band at 804 nm is attributable to the Q_y transitions of the monomeric BChls, together with a contribution from the high energy exciton component of the Q_y transition of P (B Q_y band). Finally, the band at 867 nm is attributable to the low energy exciton component of the Q_y transition of the P BChls (P Q_y band). The mutations did not have any significant effect on the H and B Q_y bands at room temperature, but the maximum of the P Q_y absorbance band was shifted from 867 nm in the membrane-bound wild-type reaction centre, to between 859 and 845 nm in the mutant complexes (Table 1). There was also a decrease in the relative intensity of the P Q_y band. Similar changes in the properties of the P Q_y band were also observed in spectra of membrane-bound reaction centres recorded at 30 K (Table 1). The absorbance region between 530 and 600 nm was not analyzed, because light scattering by membranes distorts the absorbance bands in this spectral region.

To study the effect of the mutations in more detail, absorbance spectra were recorded at 30 K for reaction

Table 1

Mutation	Maximum of P Q_y band (nm)			Maximum of P^+ band (nm)	E_m P/P^+ (mV)
	RT—membranes	30 K—membranes	30 K—purified reaction centres	30 K—purified reaction centres	RT—membranes
Wild-type	867	898	894	1245	493
HL168L	859 (−8)	890 (−8)	892 (−2)	1256 (+11)	370 (−123)
HL168D	856 (−11)	883 (−15)	877 (−17)	1253 (+8)	402 (−91)
HL168F	850 (−17)	875 (−23)	871 (−23)	1241 (−3)	378 (−115)
HL168K	845 (−22)	879 (−19)	870 (−24)	1253 (+8)	407 (−86)
HL168R	845 (−22)	875 (−23)	870 (−24)	1262 (+17)	433 (−60)

centres that had been purified from antenna-deficient membranes (Fig. 2). With one exception, detailed below, the solubilization and purification process had only minor effects on the reaction centre Q_y bands. For the purposes of comparison, the spectra in Fig. 2 were normalized to the same amplitude of the H Q_y band at 759 nm, which was least affected by the mutations. At 30 K, the absorbance maximum of the P Q_y band of the purified wild-type reaction centre was at 894 nm. In the mutant complexes this band was shifted to the blue by an approximately equal amount in both purified (Fig. 2 and Table 1) and membrane-bound reaction centres (Table 1). The one exception to this agreement was the HL168L reaction centre, which showed an 8-nm blue-shift of the P Q_y band in membrane-bound reaction centres at 30 K (and room temperature), but only a 2-nm blue-shift of the band in purified reaction centres at 30 K. Again, the relative intensity of the P Q_y band appeared to be decreased in the spectra of the mutant reaction centres (Fig. 2 and Table 1).

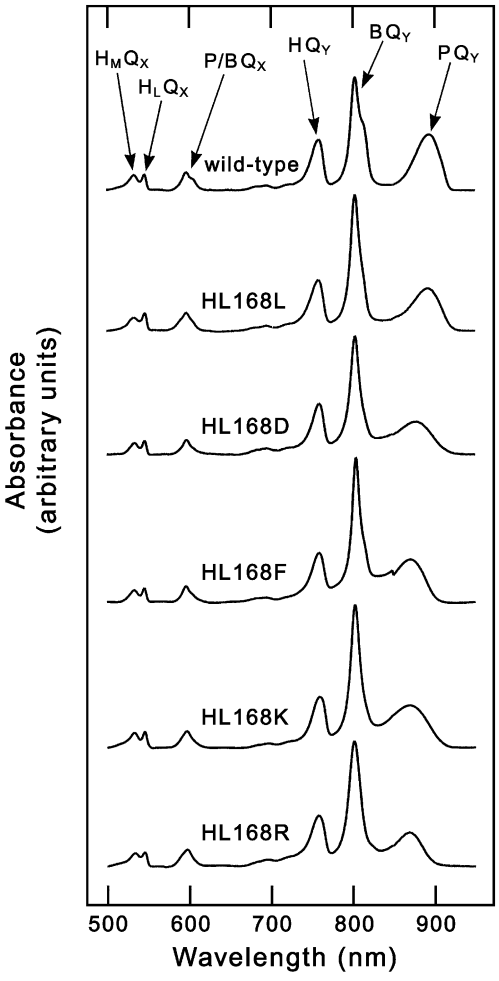

Fig. 2. Absorbance spectra of wild-type and mutant reaction centres, recorded at 30 K. Spectra were normalized to the amplitude of the H Q_y band at 759 nm.

The mutations also all had an effect on the B Q_y band, which in the wild-type reaction centre exhibits more structure at low temperature than at room temperature. In the wild-type reaction centre at 30 K, the B Q_y band has a maximum at 803 nm, usually attributed to the Q_y transition of the L-branch monomeric BChl (B_L) and a pronounced shoulder at approximately 814 nm, usually attributed to the Q_y transition of the M-branch monomeric BChl (B_M) and/or the high energy exciton component of the Q_y transition of P (Fig. 2). In spectra recorded at 30 K for both membranes (not shown) and purified reaction centres (Fig. 2) from the mutant strains, the absorbance giving rise to the shoulder on the red side of the B Q_y band was largely lost, and there was an increase in the relative amplitude of the main band at 803 nm. The mutations also affected the asymmetric absorbance band with a maximum at 597 nm that is attributed to the Q_x transitions of all four reaction centre BChls (P/B Q_x bands). The general effect of the mutations was to cause loss of the shoulder visible on the red side of this band at approximately 605 nm in the spectrum of the wild-type reaction centre (Fig. 2). The mutations did not affect the position of the H Q_y band at 759 nm, or the Q_x bands of H_M and H_L at 533 and 546 nm, respectively.

Upon either chemical or photochemical oxidation of P, a new absorbance band is observed at approximately 1245 nm, that has been attributed to the cation radical of the P dimer, P^+ [36–38]. All of the mutations studied affected both the energy and intensity of this P^+ band, in spectra of chemically oxidized, purified reaction centres recorded at 30 K (Fig. 3 and Table 1).

3.2. Effects on the electrochemical properties of P

Published studies have shown that, in the purified HL168F reaction centre, breakage of the hydrogen bound donated to the acetyl carbonyl of P_L is accompanied by a 95 mV decrease in E_m P/P^+ [15,17]. Values of E_m P/P^+ were determined for the membrane-bound wild-type reaction

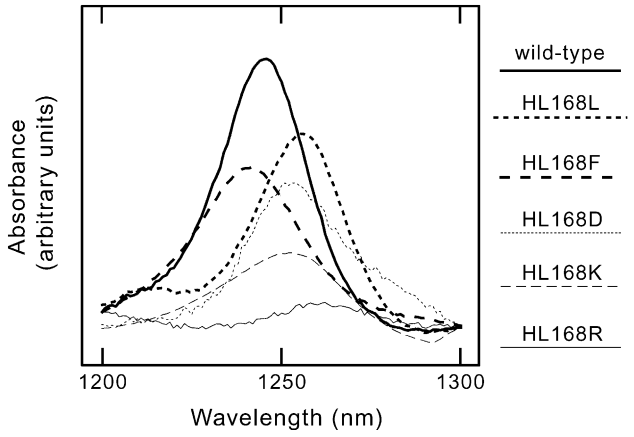

Fig. 3. Spectra of chemically oxidized wild-type and mutant reaction centres, recorded at 30 K. Spectra were normalized to the amplitude of the H Q_y band at 759 nm (not shown).

centre and the five mutant complexes, as described in Materials and methods, and are shown in Table 1. The HL168F and HL168L reaction centres showed very strong reductions in E_m P/P^+ (-115 and -123 mV, respectively, relative to the wild-type reaction centre). The mutations HL168K and HL168D also resulted in a strong (>85 mV) reduction in E_m P/P^+, whilst the HL168R mutation brought about a 60 mV decrease in E_m P/P^+.

3.3. FT-Raman spectroscopy of the P BChls

To investigate the effect of the mutations on hydrogen bonding, FT Raman spectra were recorded for ascorbate-reduced, purified reaction centres (Fig. 4). Measurements were made with 1064-nm excitation, as described in Materials and methods. In the carbonyl stretching region, the FT-Raman spectrum of the wild-type reaction centre contains a band at 1620 cm^{-1} (indicated by the arrow in Fig. 4) that has been attributed to the acetyl carbonyl of P_L, hydrogen bonded to His L168 [17]. Previous studies on the HL168F mutant have shown that, on removal of the hydrogen bond donor, this band up-shifts in frequency and underlies a band at 1653 cm^{-1} that has been attributed to the non-bonded acetyl carbonyl of P_M [17]. This change is accompanied by an increase in intensity of the band at 1680 cm^{-1}, which is attributed to the keto carbonyl of P_M [17]. The increase in intensity of the 1680 cm^{-1} band is caused by a 3 cm^{-1} down-shift of a band at 1691 cm^{-1} in the spectrum of the wild-type reaction centre, attributed to the keto carbonyl of P_L. The HL168F mutation therefore causes a strong up-shift of the stretching frequency of the acetyl carbonyl group of P_L, and a weak down-shift of the stretching frequency of the keto carbonyl of P_L [17]. The same changes in spectrum were recorded for the purified HL168F reaction centre in this study (Fig. 4).

The changes in spectrum caused by the HL168L (Fig. 4) and HL168K (not shown) mutations were essentially identical to those observed for the HL168F reaction centre. This provides direct evidence for the breakage of the hydrogen bond to the acetyl carbonyl of P_L in both of these reaction centres.

In the case of the HL168R reaction centre, there was also a loss of the 1620 cm^{-1} band and an increase in intensity in the region of the 1653 cm^{-1} band (Fig. 4). However, in this case a new, rather weak band was also observed at 1632 cm^{-1}. This may have arisen from an up-shift of all or part of the 1620 cm^{-1} band (see Discussion). The 1632 cm^{-1} band was not present in the FT-Raman spectrum the oxidized HL168R reaction centre (data not shown), which would suggest that it was genuinely associated with the ground state of P and not a background contribution.

Interpretation of the spectrum of the HL168D reaction centre was also not straightforward. Although there was again a down-shift of the 1693 cm^{-1} band and clear loss of the 1620 cm^{-1} band, which could indicate breakage of the hydrogen bond from the L168 residue to P, there was no clear accompanying increase in intensity at 1653 cm^{-1}. Possible reasons for this result are considered in the Discussion.

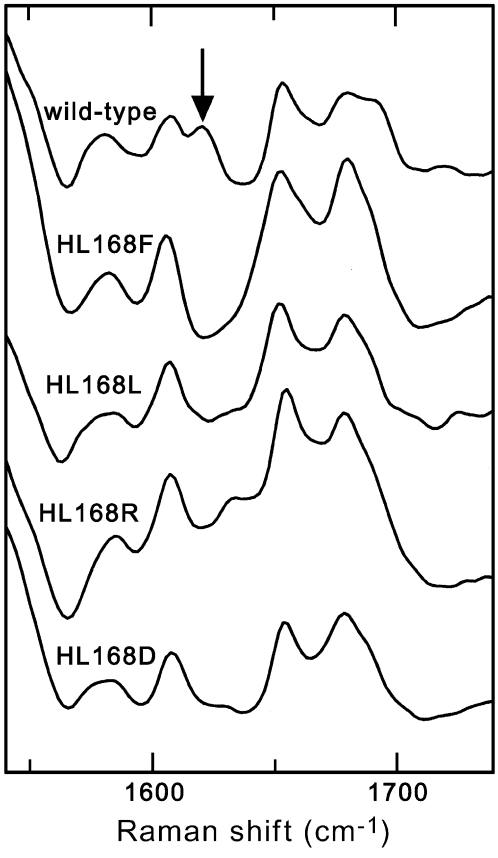

Fig. 4. FT Raman spectra of ascorbate-reduced, purified reaction centres. The arrow indicates the band at 1620 cm^{-1} in the spectrum of the wild-type reaction centre that is attributed to the acetyl carbonyl of the P_L BChl, hydrogen bonded to His L168.

3.4. FTIR spectroscopy of the P BChls

Light-induced FTIR difference spectra were recorded for membrane-bound wild-type and HL168F reaction centres. The spectra shown in Fig. 5A, which were measured for antenna-deficient membranes, were similar to spectra published previously for wild-type and HL168F reaction centres in antenna-containing membranes [13]. Overall, the ($P^+Q_A^-$)-minus-(PQ_A) spectrum obtained for the HL168F complex was closely comparable to that of the wild-type reaction centre in the 1800–1200 cm^{-1} spectral range (Fig. 5A), showing that no large scale structural rearrangement had occurred upon mutation. However, several small changes were reproducibly observed in the carbonyl stretching region between 1600 and 1750 cm^{-1}. Notably, the small negative band at 1620 cm^{-1} in the spectrum of the wild-type reaction centre (indicated by the asterisk), which has been proposed to correspond to the acetyl carbonyl of P_L hydrogen bonded to His L168 [13], was lacking in the spectrum of the mutant. In addition, the negative band at 1692 cm^{-1} in the spectrum of the wild-type reaction centre, which has been attributed to the keto carbonyl of P_L [39], was down-shifted by 2–3 cm^{-1} in the spectrum of the HL168F mutant. Both of these observations were fully consistent with the results of FT-Raman spectroscopy (Fig. 4), which were obtained on isolated reaction centres. In the FTIR spectra, the shoulder at 1714 cm^{-1}, assigned to the keto carbonyl of the P_L^+ state of the wild-type [39], also experienced a frequency down-shift in the mutant and merged with the keto carbonyl of the P_M^+ state, leading to a main positive feature peaking at 1705 cm^{-1}. Such perturbations of the keto carbonyl of P_L and P_L^+ can be related to small molecular rearrangements of the BChl macrocycles and/or their substituents occurring upon mutation, compounded by the sensitivity of the frequency of the keto carbonyl to the local amino acid environment and the charge density on ring V of the BChl [40].

In the 1200–1600 cm^{-1} region, three bands are present at ~1290, 1480 and 1550 cm^{-1} (indicated by arrows in Fig. 5A). These signals are, for a large part, marker bands for the *dimeric* P^+ cation [41,42], and have been assigned to phase phonon bands reflecting porphyrin modes [38]. In the HL168F reaction centre the relative intensity of each of these bands was somewhat decreased, notably for the high-frequency component of the band at ~1290 cm^{-1}. In

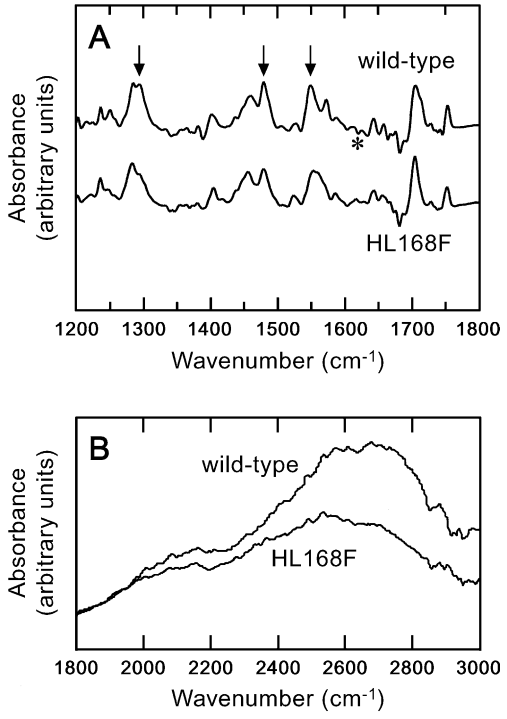

Fig. 5. Light-induced FTIR difference spectra of membrane-bound reaction centres at 100 K. The arrows indicate bands at 1290, 1480 and 1550 cm^{-1} in the spectrum of the wild-type reaction centre that are marker bands for the dimeric P^+ cation, and that are diminished in intensity in the spectrum of the HL168F mutant. The asterisk denotes the negative band at 1620 cm^{-1} characteristic of the P_L acetyl carbonyl.

Table 2
Crystallographic statistics for data collection and refinement

	HL168F RC
Collection statistics	
Number of unique reflections	71126
Completeness[a]	94.5% (97.2%)
Multiplicity	3.2 (3.0)
Rmerge[a,b]	11.2% (77.8%)
Refinement statistics	
Resolution range	27.0 – 2.50 Å
R factor[c]	17.26%
Free-R factor[d]	19.39%
Average B-factor for buried atoms[e]	29.6 $Å^2$
Geometry	
RMSD from ideality	
bonds	0.018 Å
angles	1.8°
Ramachandran plot, residues in:[f]	
Most favoured areas	93.0%
Additional allowed areas	6.8%
Generously allowed areas	0.3%
Disallowed areas	0.0%
Coordinate error[g]	0.20 Å
Model	
Number of protein residues	823
Number of cofactors	4 BChl, 2 BPhe, 2 Ubi, 1 Spo, 1 Fe
Number of waters	264
Number of detergents	9
Number of phosphates	0

[a] Figures within brackets refer to the statistics for the outer resolution shell (2.54–2.50 Å).

[b] $Rmerge = \Sigma_h \Sigma_i |\langle I(h)\rangle - I(h)_i| / \Sigma_h \Sigma_i I(h)_i$ where $I(h)$ is the intensity of reflection h, Σ_h is the sum over all reflections, Σ_i is the sum over all i measurements of reflection h.

[c] R-factor is defined by $\Sigma \| F_O| - |F_C| / \Sigma |F_O|$.

[d] Free-R was calculated with 5% reflections [76] selected to be the same as in the wild-type RC refinement [25].

[e] Calculated by the program WHAT CHECK [77].

[f] Ramachandran plot was produced by Procheck version 3.0 [78].

[g] Coordinate error was estimated by Cruickshank's DPI [79].

addition, the broad electronic transition at 2600 cm^{-1}, also characteristic of the dimeric nature of P^+, showed a strong decrease in intensity and a down-shift of ~ 100 cm^{-1} when the spectrum of the mutant complex was compared to that of the wild-type reaction centre (Fig. 5B). This band has been assigned to the hole transfer transition $P_M P_L^+ \rightarrow P_M^+ P_L$ (see Discussion), and reflects the magnitude of the resonance interactions between the two BChls of P^+ [41,43].

3.5. X-ray crystal structure of the HL168F reaction centre

The structure of the HL168F reaction centre was determined to a resolution of 2.5 Å by X-ray crystallography, as described in Materials and methods. Data collection and refinement statistics are shown in Table 2. The structural model of the HL168F reaction centre was compared with that of the wild-type complex, determined previously [25]. This comparison showed that there was good structural conservation throughout the bulk of the protein–cofactor system. The root mean square displacement calculated with program LSQKAB [44] for the main-chain atoms of the L-, M- and H-polypeptide chains in the two structures was 0.27 Å. Significant changes in structure were confined to the side-chain of the L168 residue and to the cofactors in the immediate vicinity of this residue.

Fig. 6 shows the electron density attributable to the L168 residue and part of the P_L BChl, in the maps obtained for the HL168F reaction centre, and the fit of the structural model to the density. Fig. 7 shows parts of a superimposition of the structural models of the HL168F and wild-type reaction centres, achieved using the program LSQKAB [44]. Replacement of His L168 by Phe was not accompanied by any significant deformation of the backbone at the L168 position, or at adjacent positions (Fig. 7A and B). The mutant Phe residue was only approximately co-planar with the wild-type His residue (Fig. 7B), the His and Phe rings in the two models being at a mutual angle of approximately 20°. As there was no deformation of the backbone, the centre of the Phe L168 ring was shifted by some 1.1 Å with respect to the centre of the His L168 ring in the wild-type reaction centre, in a direction towards the P_L BChl (Figs. 7 and 8).

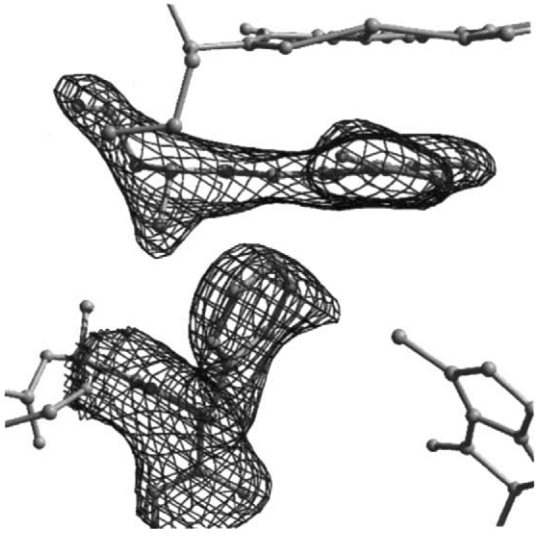

Fig. 6. Part of a $2mF_o-DF_c$ electron density map showing density attributable to Phe L168 and the P_L BChl, with the fitted structural model. The view is down the axis of the C2a–C2 bond of the P_L BChl.

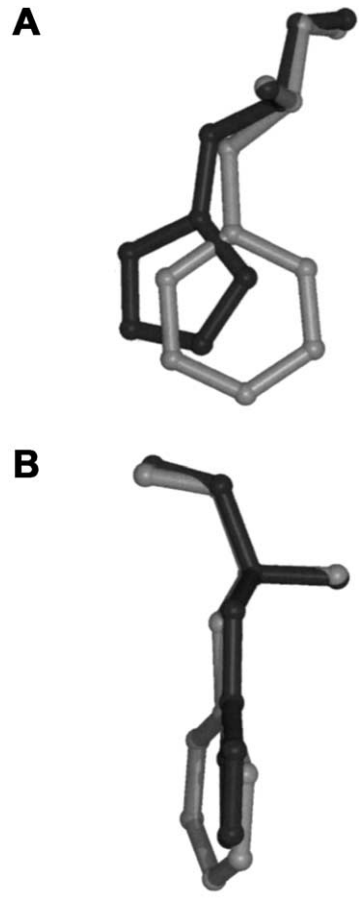

Fig. 7. Superimposition of the structural models of the wild-type (dark) and HL168F (light) reaction centres. (A) Face-on view of residue His L168 in the wild-type reaction centre and Phe L168 in the HL168F reaction centre; (B) view of the same pair along the plane of the His ring.

In the wild-type reaction centre, the NE2 nitrogen of residue His L168 is located approximately 2.7 to 3.0 Å from the carbonyl oxygen of the P_L BChl, and a hydrogen bond connects the two [17,19]. In the structure of the HL168F reaction centre, replacement of His L168 by Phe removed the possibility of this hydrogen bond, in full agreement with conclusions from vibrational spectroscopy that the hydrogen bond is abolished by this mutation [13,17,19].

Introduction of the bulkier Phe residue was accommodated by movement of that part of the macrocyle of the P_L BChl nearest residue Phe L168, in a direction away from the L168 residue and towards the P_M BChl (Fig. 8A). This movement had components that were both parallel and

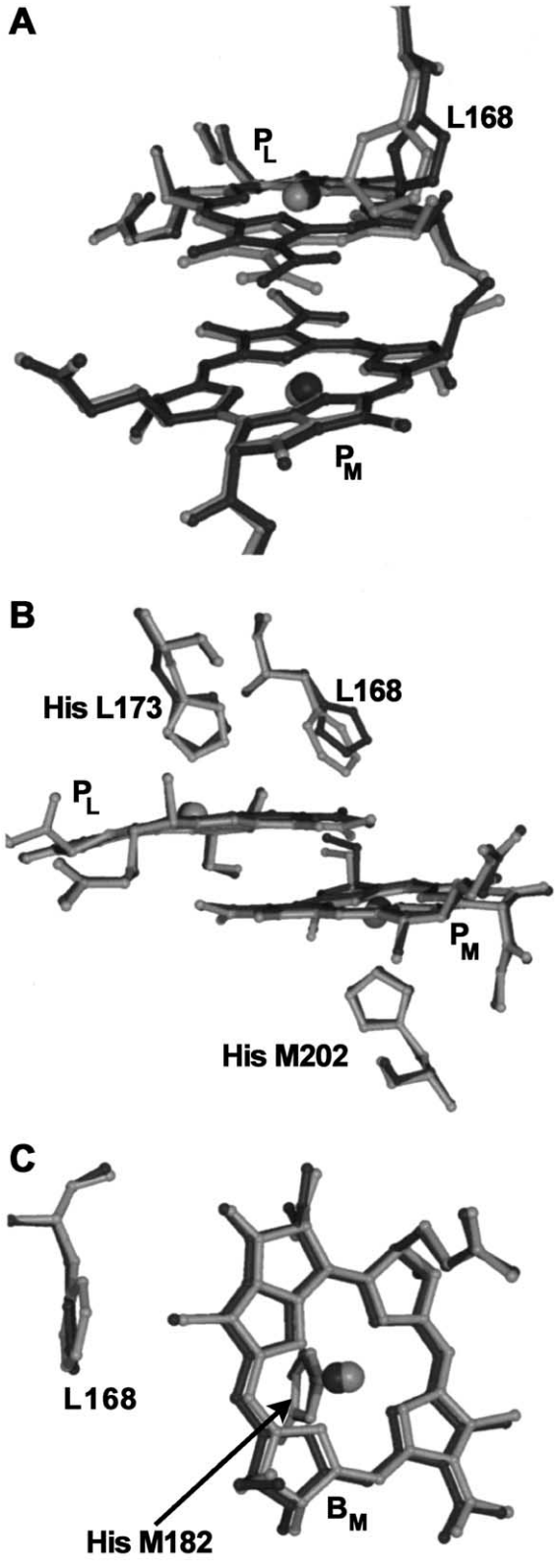

Fig. 8. Superimposition of the structural models of the wild-type (dark) and HL168F (light) reaction centres. (A) View of the P BChls and the L168 residue; (B) edge-on view of the P BChls, showing the L168, L173 and M202 residues; (C) face-on view of the B_M BChl, showing the L168 and M182 residues.

perpendicular to the plane of the BChl macrocycle. Although this movement was small, maximally approximately 0.5 Å for the carbon atoms of ring I of the P_L BChl, it was clearly apparent from the comparison of the structural models of the wild-type and HL168F reaction centres (Fig. 8A). The movement had two main effects on the overall conformation of the P BChls. First, it decreased the spacing between rings I of the P_L and P_M halves of the dimer, by between 0.1 and 0.3 Å (Fig. 8A). Second, because the movement mainly affected rings I and II of the P_L macrocycle, it increased the extent to which this macrocycle deviates from a planar conformation [3] (i.e. it increased the extent to which the P_L BChl is domed) (Fig. 8B). There was also some indication of a small movement of the P_M BChl in a direction away from the P_L BChl (maximally 0.25 Å), although this small shift was less clear (Fig. 8B). Finally, the movement of the P_L macrocycle also contributed to a change in the position and conformation of the P_L acetyl carbonyl group, as described in detail in the next section.

The His to Phe mutation also affected the macrocycle of the B_M BChl, which underwent an approximately 0.3 Å shift in position, in a direction parallel to the plane of the BChl macrocycle and away from the L168 residue (Fig. 8C). This movement was required to avoid an unreasonably close contact (estimated from the superimposed structures as being 2.7 Å) between the ring of Phe L168 and the 5A methyl carbon of the B_M BChl. In the mutant, the closest approach between the two was 3.0 Å, which was still much shorter than the 3.6 Å spacing between this methyl group and the ring of His L168 in the wild-type reaction centre. The movements of the macrocycles of P_L and B_M were accompanied by small shifts in the positions of residues His L173 and His M182, respectively, that provide the fifth, axial ligand to the central magnesium of the BChl (Fig. 8B and C).

3.6. Conformation of the acetyl carbonyl of P_L in the wild-type reaction centre

As is discussed in more detail below, it has been suggested that one of the effects of replacement of His L168 by Phe could be to elicit an in-plane rotation of the acetyl carbonyl of the P_L BChl, as a result of removal of the hydrogen bond that holds this group markedly out-of-plane in the wild-type reaction centre [14,18–20]. The assignment of a markedly out-of-plane conformation for this acetyl group in the wild-type reaction centre was made on the basis of a 2.6 Å resolution X-ray crystal structure for the reaction centre from *Rb. sphaeroides* strain R-26, described by Ermler et al. (PDB code 1PCR) [3,4]. The angle of the C2a=O carbonyl bond relative to the plane of the BChl macrocycle can be expressed as the C12–C2–C2a–O dihedral angle (ϕ_{Ac}), carbons C2 and C12 forming part of ring I of the macrocycle (Fig. 1A). The model of the acetyl carbonyl of P_L in the 1PCR coordinates gives

$\phi_{Ac} = 88°$, indicating an almost fully out-of-plane conformation. However, this value is markedly different to that in all of the comparable structures for the *Rb. sphaeroides* reaction centre deposited in the Protein Structure Database. A survey of 11 structures at a resolution of 2.7 Å or better, present in the Structure Database as of December 2001, yielded a range of values for ϕ_{Ac} between $-2°$ and $21°$ (the distance between the carbonyl oxygen and the NE2 nitrogen of His L168 varies between 2.7 and 3.0 Å in these structures). A number of these structures are for mutant reaction centres, but in each case the mutation(s) are not expected to affect the conformation of the P_L BChl, or residue His L168.

In a recent description of a 2.1 Å resolution X-ray crystal structure of an AM260W mutant reaction centre, which was based on electron density maps of particularly high quality, we reported values of ϕ_{Ac} for the acetyl carbonyl groups of all of the reaction centre BChls and BPhes [45]. The AM260W mutation is near the binding site of the Q_A ubiquinone, and does not affect the conformation of the reaction centre BChls or BPhes, the absorbance spectrum of these cofactors, or the kinetics of primary electron transfer from P* to the H_L BPhe [45,46]. Modeling of the conformation of the bacteriochlorin acetyl groups in this structure was assisted by the relatively high quality and resolution of the data. In this structural model, ϕ_{Ac} for the acetyl carbonyl of P_L was $13°$, approximately in the middle of the $-2°$ to $21°$ range outlined above. This is close to the value of $11°$ that we estimate for this group in our structural model of the wild-type reaction centre [25].

In the case of the HL168F reaction centre described in this report, the structural model gave a better fit to the electron density if it was assumed that the acetyl group of the P_L BChl had undergone a $27°$ ''through-plane'' rotation relative to the conformation in the wild-type reaction centre (see below). This change was favoured over an approximately $150°$ flip, as modelling this acetyl group with the 2b methyl group pointing towards Phe L168 resulted in an unrealistically close approach between the two. Replacement of His L168 by Phe thus appeared to have pushed this acetyl group below the plane of the BChl ring, such that ϕ_{Ac} becomes $-16°$ in the structural model of the HL168F reaction centre (Fig. 8A). The extent to which the acetyl group is oriented out-of-the-plane of the BChl ring is therefore comparable in the two structures, but the acetyl group has undergone a $27°$ through-plane rotation relative to the conformation in the wild-type reaction centre.

The combined effects of the HL168F mutation on the P_L BChl resulted in an approximately 1.1 Å movement of the carbonyl oxygen, in a direction away from the L168 side-chain (Fig. 8A). The distance between the carbonyl oxygen and the CZ carbon of the ring of Phe L168 was 3.2 Å, longer than the corresponding distance between the carbonyl oxygen and the NE2 nitrogen of His L168 in the wild-type reaction centre (see above). The 2b methyl carbon underwent a 0.6 Å shift in position as a result of the mutation.

As mentioned above, the structural model of the HL168F reaction centre supports the conclusion from FTIR and FT-Raman spectroscopy, that this mutation abolishes the hydrogen bond between the acetyl carbonyl of P_L and the surrounding protein. However, as a result of the through-plane rotation of the acetyl carbonyl of P_L there was a decrease in the distance between the carbonyl oxygen and the magnesium of the P_M BChl. In the wild-type reaction centre this distance was 4.1 Å, but it was reduced to 3.2 Å in the HL168F mutant (Fig. 8A). Although this change in structure would make an interaction between the acetyl carbonyl oxygen of P_L and the magnesium of P_M more feasible, it should be noted that there is no indication from FT-Raman spectroscopy that the HL168F mutation affects the 5-coordinated status of the P BChls, either in their ground or cation state [19].

3.7. Other aspects of the X-ray structure of the HL168F mutant

In a recent publication, we attributed electron density at the intra-membrane surface of a reaction centre with the mutation AM260W to a molecule of the diacidic phospholipid cardiolipin [26], and we also modeled this lipid molecule in a recent X-ray structure of a YM210W mutant reaction centre [47]. In the present case we did not model this lipid because the relevant electron density was incomplete, in line with previous findings (see discussion on this point in Refs. [26,48]). The factors that determine whether full or partial density is observed for this lipid is the subject of an ongoing investigation. The final structural model of the HL168F reaction centre did include nine detergent molecules, modeled into elongated electron density features elsewhere on the intra-membrane surface of the protein. At present we cannot discount the possibility that the features we have modeled as detergents actually correspond to the acyl chains of partially resolved lipids.

The Q_B ubiquinone was also included in the final structural model of the HL168F reaction centre, with an occupancy of approximately 0.5 (based on a comparison of B-factors). The conformation adopted by the ubiquinone was similar to that described in detail for this cofactor in a recent report on the X-ray structure of the AM260W mutant [45].

4. Discussion

Mutations at the L168 position clearly have significant effects on the optical and electrochemical properties of the P dimer. Before discussing these, we briefly discuss other significant effects of the L168 series of mutations, and compare our results with a recently reported structure for a HL168F mutant of the *Rps. viridis* reaction centre.

4.1. Effects of the mutations on the optical properties of the monomeric BChls

Replacement of the L168 histidine brings about a change in the characteristics of the B Q_y band at cryogenic temperatures. At 30 K, the B Q_y band in the spectrum of the wild-type reaction centre is asymmetric, with a main peak at 800 nm and a pronounced shoulder on the red side at approximately 814 nm. The former is usually attributed to the Q_y transition of the B_L BChl, whilst the latter is attributed to the Q_y transition of the B_M BChl and/or the high energy exciton component of the P Q_y transition. In the HL168F mutant, it has been reported that this shoulder is absent, and the main band at 800 nm increases in intensity [17]. This result was reproduced for the HL168F mutant in the present study, and was also observed for the four new mutations at this position.

This shift has previously been attributed to an effect of the HL168F mutation on the absorbance properties of P [17]. However, in the light of the findings described above, an alternative possibility is that this effect is due to a change in the absorbance properties of the B_M BChl, which shifts its position slightly in response to the His to Phe mutation at L168.

4.2. Effects of the HL168F mutation on coherent vibrational modes coupled to the P* state

Transmembrane electron transfer is driven from the first singlet excited state of the primary donor, denoted as P*. In recent years it has been shown that the fluorescence properties of this excited state on the picosecond time-scale are modulated by coherent nuclear motion (see Refs. [49,50] for reviews). The molecular origin of these vibrational modes is not known, but their low frequency (30–200 cm^{-1}) suggests that they involve the protein as well as the BChls of the P dimer. In a recent study, Rischel et al. [51] showed that the frequency spectrum of these P*-coupled vibrational modes is altered by mutation of His L168 to Phe. The spectrum of the wild-type reaction centre showed main bands at 62, 94 125 and 156 cm^{-1}, but in the HL168F reaction centre the main modes were at 39, 117, 133 and 172 cm^{-1}. This spectrum was also strongly affected if the symmetry related residue Phe M197 was mutated to His, introducing a new hydrogen bond to the acetyl carbonyl of the P_M BChl, but much weaker effects were seen if a new hydrogen bond was introduced to the keto carbonyl of P_L [51]. The conclusions of this study were that the frequency of the vibrational modes coupled to the P* state are particularly sensitive to mutations near the acetyl carbonyl groups, which are near the interface between P_L and P_M in the P dimer (Fig. 1B), but are much less sensitive to changes near the edges of the dimer [51].

The X-ray crystal structure of the HL168F mutant shows, within the limits imposed by the resolution of the data, that changes in the structure of the protein–cofactor system are largely limited to the interface region between P_L and P_M halves of the dimer, and that the changes in structure that occur are small. We can therefore exclude the possibility that the observed changes in the frequency spectrum of the P*-coupled vibrational modes caused by the HL168F mutation are due to gross changes in the structure of the P dimer or its protein environment. The changes in structure observed suggest two possible sources for the effects reported by Rischel et al. [51]. The first is a change in the conformational freedom of the acetyl carbonyl of the P_L BChl, caused by the substitution of His by a more bulky Phe, which could affect the frequency of in-plane and out-of-plane deformations associated with this group [52]. The second is a change in the detailed conformation of the P_L macrocycle and the overlap between the two halves of the P dimer, again caused by the substitution of His by a more bulky Phe, which could affect low frequency modes associated with the BChl dimer [51].

4.3. Structural comparisons with the HL168F mutant of the Rps. viridis reaction centre

The HL168F mutation has also been constructed in the *Rps. viridis* reaction centre. In this species the mutation produces an 80 mV decrease in E_m P/P^+, and a 35-nm blue-shift of the P Q_y band [53]. The structure of the *Rps. viridis* mutant has recently been described, to a resolution of 2.0 Å [54] and the structure shows a number of similarities to the structure of the *Rb. sphaeroides* mutant described in this report. In both structures, the His to Phe mutation does not produce any deformation of the backbone at the L168 position, or at adjacent positions. In both structures the Phe side-chain occupies a position that is similar to the wild-type His residue, but because Phe is larger than His it causes a distinct shift in the position of the P_L BChl, affecting in particular ring I of the bacteriochlorin (maximally 0.4 Å in the *Rps. viridis* structure). In *Rps. viridis*, the acetyl carbonyl group is described as having undergone a 20° rotation, which moves the group away from Phe L168 and through the plane of the BChl macrocycle; this change in conformation is similar to that described above for the *Rb. sphaeroides* mutant. Our conclusion is that there are no marked differences in the structural consequences of the mutation when the two species are compared.

The HL168F mutation has essentially no effect on the rate of primary electron transfer in the *Rb. sphaeroides* reaction centre, as determined from the lifetime of the P* state. This lifetime is reported as being 3.6 ps in the HL168F mutant, compared to 3.5–3.8 ps measured for the wild-type reaction centre [14,18]. In marked contrast, this mutation produces a significant acceleration in the rate of primary electron transfer in the *Rps. viridis* reaction centre, changing the lifetime of the P* state from 3.5 ps to a remarkable 1.1 ps [53]. This marked difference occurs despite the fact that the mutation produces a similar decrease of E_m P/P^+ in the two species. The X-ray structure of the *Rps. viridis* mutant

did not yield any obvious reason as to why the HL168F mutation produces such a strong acceleration in the rate of primary electron transfer [54]. Lancaster and co-workers did comment on a very small decrease in the distance between the P_M BChl and the B_L BChl, which could indicate an increased electronic coupling between the two that might contribute to the accelerated rate of P* decay. This separation was measured between the C2B atom of the P_M BChl and the C2D atom of the B_L BChl, and was reduced from 5.45 Å in the wild-type reaction centre to 5.3 Å in the HL168F mutant. However, as pointed out by Lancaster and co-workers, this 0.15 Å difference was as large as the estimated position error in their 2.0 Å structure. In our data we found this distance to be approximately 5.8 Å in both the wild-type complex and in the HL168F mutant (with the estimated coordinate error for our structure of 0.20 Å). Our data therefore provides a possible explanation for why the lifetime of the P* state is unaffected by the HL168F mutation in the *Rb. sphaeroides* reaction centre, but is dramatically shortened by this mutation in the *Rps. viridis* reaction centre.

4.4. Changes in hydrogen bonding on replacement of His L168

We now turn to the effects of the mutations on the properties of the P dimer. It is known from published FTIR and FT-Raman spectra [13,17] that mutation of His L168 to Phe abolishes the hydrogen bond interaction between the acetyl carbonyl of P_L and the surrounding protein. This finding was reproduced in the present work (Fig. 4), which showed in addition that the mutations HL168L and HL168K also abolish this hydrogen bond. In all three mutants, the stretching frequency of the acetyl carbonyl of P_L appeared to shift from 1620 to 1653 cm^{-1}. For the HL168F mutant the conclusion that this carbonyl group is no longer hydrogen bonded was supported by the X-ray crystal structure, which showed that the His to Phe mutation removes the only group that is in hydrogen bond distance of the acetyl carbonyl of P_L. As described in the Results, the crystallographic data argue against the possibility that the acetyl carbonyl of P_L is bonded to the magnesium of the P_M BChl in the HL168F mutant, in line with the same conclusion from FT-Raman spectroscopy [19].

Interpretation of the FT-Raman spectrum of the HL168R reaction centre was not straightforward. In the absence of other considerations, the loss of the 1620 cm^{-1} band and the appearance of a new contribution at 1632 cm^{-1} suggested a decrease in the strength of the hydrogen bond to the acetyl carbonyl of P_L. However, the 1632 cm^{-1} band was relatively weak, and there also appeared to be extra intensity associated with the 1653 cm^{-1} band. Taken together, these observations could indicate that the HL168R reaction centres are heterogeneous, with one population having a weak hydrogen bond to the acetyl carbonyl of P_M which gives rise to the 1632 cm^{-1} band, and a second with no hydrogen bond giving rise to the extra intensity at 1653 cm^{-1}.

Recently, we have published the X-ray crystal structure of a reaction centre with a Phe to Arg mutation at the M197 position, the symmetry-related residue to His L168 [25]. In that crystal structure, it was evident that the Arg M197 residue does not interact with the P BChls, but rather points away from the P BChls and towards the periplasmic surface of the protein, where it interacts with Asp L155. The reorientation of Arg M197 creates a cavity adjacent to the P_L BChl that contains at least two new water molecules, and one of these appears to form a hydrogen bond to the acetyl carbonyl group of the P_M BChl. In the light of these findings, it seems prudent to consider the possibility that a mixed population of HL168R mutant reaction centres could arise from heterogeneity in the conformation of the Arg L168 residue and/or heterogeneity in the arrangement of bound water molecules in this region of the protein.

The hydrogen bonding status of the P_L acetyl carbonyl group in the HL168D reaction centre was also not clear from the FT-Raman spectrum. It is known that acidic amino acids can form hydrogen bonds to bacteriochlorin carbonyl groups. In the wild-type reaction centre, the keto carbonyl of the L-branch BPhe is hydrogen bonded to residue Glu L104 [55,56]. Furthermore, mutation of residue Leu M160 to either Asp or Glu results in the formation of a moderate strength hydrogen bond with the keto carbonyl of P_M [57]. Recently, we have also shown that an Asp mutation at residue Phe M197, which is the symmetry-related residue to His L168, results in the formation of a relatively weak hydrogen bond with the acetyl carbonyl of P_M [58]. In the present case, the FT-Raman spectrum of the HL168D reaction centre was somewhat ambiguous (Fig. 4), in that although the band at 1620 cm^{-1} was lost and there was a 4 cm^{-1} down-shift of the 1693 cm^{-1} band, there was no pronounced increase in intensity in the region of 1653 cm^{-1} that should accompany breakage of the hydrogen bond to the acetyl carbonyl of P_L. Circumstantial evidence that this hydrogen bond is in fact lost or significantly weakened in this mutant comes from the 91 mV decrease in E_m P/P^+ measured for the HL168D reaction centre.

One possible explanation for the apparent loss of the contribution of the P_L acetyl carbonyl from the FT-Raman spectrum of the HL168D reaction centre is that the carbonyl group is no longer conjugated to the π electron system of the P BChls in this mutant. A property of this carbonyl group is that, in principle, it can rotate relative to the plane of the bacteriochlorin ring around the C_2-C_{2a} bond (Fig. 1). It has been proposed that the strength of the coupling of the carbonyl bond to the π electron system of the bacteriochlorin ring is dependent upon the orientation of the carbonyl group, decreasing as the group is rotated out-of-plane [11]. As FT-Raman spectroscopy, as applied in our experiments, is selective for vibrational modes that are coupled to the P Q_y optical transition, it is possible that an out-of-plane rotation of the acetyl carbonyl group of P_L

on mutation of His L168 to Asp would cause loss of the stretching frequency of this carbonyl group from the FT-Raman spectrum. Although this explanation would account for the net loss of the contribution of the acetyl carbonyl group of P_L, it of course does not throw any light on the issue of whether Asp L168 donates a weak hydrogen bond to this group, and the strength of that bond. We recently put forward the same explanation to account for the lack of a contribution of the acetyl carbonyl of P_M to the FT-Raman spectrum of the FM197R mutant described above [58]. The X-ray crystal structure of the FM197R reaction centre shows that the mutation causes a $\sim 20°$ out-of-plane rotation of the P_M acetyl carbonyl group [25,58].

4.5. Changes in E_m P/P$^+$ on replacement of His L168

In the HL168F and HL168L reaction centres, abolition of the hydrogen bond interaction between the protein and the acetyl carbonyl of P_L was accompanied by a strong decrease in E_m P/P$^+$ (-115 and -123 mV, respectively). The change of -115 mV determined for the membrane-bound HL168F reaction centre is broadly consistent with the change of -95 mV reported for purified reaction centres containing this mutation [15]. The significant decrease in E_m P/P$^+$, observed in the HL168F mutant, has been attributed to a stabilization of the oxidized state of the primary donor as a result of removal of the dipole between the partial negative charge of the NE2 nitrogen of His L168 and the partial positive charge of the hydrogen bond proton [14].

In the HL168K reaction centre, E_m P/P$^+$ was changed by -85 mV, a smaller effect than that observed for the HL168F and HL168L reaction centres. As FT-Raman spectroscopy showed that the hydrogen bond interaction is also abolished in the HL168K reaction centre, it seems likely that the Lys residue brings about a further (30–40 mV) modulation of E_m P/P$^+$ through a nonbonding effect, presumably electrostatic in nature, that destabilizes the P$^+$ state. The size of this modulation is of the same order as changes in E_m P/P$^+$ that follow mutation of residues that are not in a position to form hydrogen bond interactions with P [14,57,59–62]. Although caution has to be applied when assuming what the structural consequences of a particular mutation may be, it seems likely that the majority of these changes in E_m P/P$^+$ arise from effects other than changes in the number and strength of hydrogen bond interactions between P and the surrounding protein. For example, no significant changes in the FT-Raman spectrum of P were seen for a set of reaction centres with mutations at the M210 position that increase E_m P/P$^+$ by as much as 50 mV [23,62], or in reaction centres with mutations at the L167, M196 or M156 position that increase E_m P/P$^+$ by up to 44 mV [57]. In the latter case, the increases in E_m P/P$^+$ were accounted for on the basis of electrostatic interactions that alter the electronic structure of P [57], although a detailed study of these interactions was not made.

Although nonbonding interactions can have sizeable effects on E_m P/P$^+$, it has also been shown that, when introduced at a suitable position such as residue M160, a wide range of polar residues (including Lys) can donate hydrogen bonds to a carbonyl group of P [57]. The strength of the hydrogen bond donated to the keto carbonyl of P_M in these experiments was shown to depend on the identity of the hydrogen bond donor, and for a set of polar residues (with the exception of His) an approximately linear relationship was observed between the change in hydrogen bond interaction energy and the change in E_m P/P$^+$ [57]. The 30–40 mV modulation of E_m P/P$^+$ seen in the HL168K reaction centre (compared with the HL168F/HL168L reaction centres) could therefore result from a weak hydrogen bond donated by Lys L168. However, the results of FT-Raman spectroscopy argue against this possibility.

The HL168D mutation produced a change in E_m P/P$^+$ of -91 mV. As for the HL168K mutant, this change could be indicative of a weak hydrogen bond interaction between the L168 residue and the acetyl carbonyl of P_L, or it could be due to an electrostatic modulation of E_m P/P$^+$. As discussed above, the FT-Raman spectrum of this mutant was difficult to interpret, and so it is not possible to distinguish between these possibilities in this case.

The smallest change in E_m P/P$^+$ was seen in the HL168R mutant (-60 mV), where again the FT-Raman spectrum was difficult to interpret. In this case there was some evidence from the FT-Raman spectrum of a weak hydrogen bond in at least part of the reaction centre population, which would be broadly consistent with the observed effect on E_m P/P$^+$. However, the FT-Raman spectrum also gave some indication of heterogeneity in the population of HL168R reaction centres, although there was no indication of a biphasic titration curve in the measurements of E_m P/P$^+$ that would support this.

The relative effects of the different mutations on E_m P/P$^+$ suggest that the polarity of the L168 residue is a relevant parameter. A detailed investigation of this including data from reaction centres with mutations at the symmetry-related M197 residue [58] will be published elsewhere (Spiedel, Jones and Robert, manuscript in preparation).

4.6. Effects of the mutations on the optical properties of P

All of the mutant reaction centres exhibited a significant blue-shift of the P Q_y band, both at room temperature and 30 K. Similar shifts have been reported for a number of reaction centres with mutations of residues in the vicinity of P [14,19,25]. A number of suggestions have been made as to the origin of the shift observed in the HL168F mutant [14,18–20]. These proposals were made largely on the basis of computational studies of the optical properties of protein-bound BChl, looking at the effect of particular changes in the structure and interactions of BChl on the absorption spectrum of the reaction centre [63,64].

One proposal is that the blue-shift of the P Q_y band is an effect of removal of the hydrogen bond between the acetyl carbonyl of P_L and His L168 [14], in accord with the predictions of calculations [63]. In all five of the mutant complexes studied in this work, loss (or weakening) of the strong hydrogen bond donated by His L168 was accompanied by a blue-shift of the P Q_y band. However, it was noticeable that there was no correlation between the observed blue-shift of this band and the change in the strength of the hydrogen bond interaction between the L168 residue and the P_L BChl. To illustrate this, mutation to Phe or Leu caused breakage of the hydrogen bond interaction and comparable reductions in E_m P/P^+ (-115 and -123 mV, respectively). However, the HL168L mutation brought about the weakest shift of the P Q_y band (8 nm) whilst the HL168F mutation brought about the strongest shift (22 nm).

An alternative proposal is that the blue-shift of the P Q_y band is caused by a "modest repositioning" of the P_L and P_M BChls relative to one another, which affects the strength of the interaction between the two [19]. As described above, the X-ray structure of the HL168F reaction centre indeed indicates a small shift in the position of the P_L BChl relative to P_M. In addition, vibrational spectroscopy has also provided indications that there is a small change in the positioning of the P_L BChl relative to its surroundings following mutation of His L168 to Phe. Both the FT-Raman [17,19] (Fig. 4) and FTIR [13] (Fig. 5) spectrum of the HL168F reaction centre show a small (3 cm^{-1}) perturbation of the stretching frequency of the keto carbonyl of P_L, which is at the opposite side of the macrocycle to the acetyl carbonyl and the L168 residue (Fig. 1). This perturbation was also evident in the FT-Raman spectra of the remaining mutants (Fig. 4). A small change in the structure of P has been cited as a possible explanation of this effect in the HL168F mutant [17]. However, it should be noted that calculations predict that a small decrease in the inter-dimer spacing, such as that indicated by the crystallographic data, would be expected to cause a red-shift of the P Q_y band [63], in contrast to the observed blue-shift.

It has also been proposed that the position of the P Q_y band could be affected by a rotation of the acetyl carbonyl of P_L, consequent on the removal of the hydrogen bond donated by His L168 [14,18–20]. In a recent publication [25], it was demonstrated from a combination of spectroscopy and X-ray crystallography that a 15-nm blue-shift of the P Q_y band in a FM197R mutant reaction centre at room temperature is accompanied by an approximately 20° out-of-plane rotation of the acetyl carbonyl group of P_M, supporting proposals that the orientation of this group relative to the plane of the bacteriochlorin ring has an influence on the absorption properties of the bacteriochlorin [63–65]. As discussed in detail above, the HL168F mutation does in fact cause a change in the orientation of the acetyl carbonyl of P_L. However, this involves a 27° through-plane rotation, rather than the significant into-plane rotation that has been discussed previously for this mutant [20,57]. Calculations suggest that a through-plane rotation of the magnitude we observe would result in a blue-shift of the P Q_y band of only a few nanometers [63,64], and therefore could account for only part of the effect seen.

Finally, it has also been pointed out that shifts in the Q_y absorption spectrum of BChl can be expected from the introduction of charged amino acids [63,65], which is an additional complication for some of the mutants described above. In addition, the possible effects of increased doming of the P_L macrocycle on the optical properties of P should also be taken into account in future analyses (see above).

4.7. Effects of the mutations on the optical properties of P^+

In addition to affecting the P Q_y band, all of the mutations also affected the characteristics of the P^+ band that is centred at 1250 nm at room temperature, and at 1245 nm in the 30 K spectrum of the oxidized wild-type reaction centre (Fig. 3). In particular, all of the mutations brought about a decrease in the intensity of this band.

A number of studies have addressed the origin of this absorption band of P^+. Verméglio and Paillotin [37] have proposed that this band is attributable to the formation of a P^+ excited state that has mixed singlet and triplet character. Shuvalov and Parson [36] have proposed that the band results from the formation of a triplet excited state on one BChl of the P^+ dimer when the other BChl of the dimer carries the charge of the cation, for example the transition $P_M P_L{}^+ \rightarrow {}^3P_M P_L{}^+$ or the transition $P_M P_L{}^+ \rightarrow P_M{}^+ {}^3P_L$, the mechanism involving coupled changes of spin on both BChls. Parson et al. [43] have presented an explanation for the 1250-nm band based upon a model in which resonance interactions between the localized, energetically inequivalent states $P_L{}^+$ and $P_M{}^+$, in which the unpaired electron resides in the highest-occupied molecular orbital (HOMO), are proposed to give rise to two nondegenerate supermolecular eigenstates, termed ψ_a and ψ_b for the low and high energy states, respectively. Similarly, resonance interactions between the localized, energetically inequivalent excited states of $P_L{}^+$ and $P_M{}^+$, in which the unpaired electron residues in the second highest-occupied molecular orbital (SHOMO), also give rise to two nondegenerate supermolecular eigenstates, termed ψ_c and ψ_d for the low and high energy state, respectively. The origin of the 1250-nm band was proposed to be an electronic transition from the ψ_a eigenstate to the ψ_c eigenstate.

Most recently, Reimers and Hush [38] and Reimers et al. [66] have presented calculations in support of the proposal that the 1250-nm band arises from the formation of a triplet state on the half of the dimer not carrying the charge of the cation [36]. The ground state of the P^+ cation is assumed to have the positive charge localized largely on the P_L BChl (Fig. 9A), and it is proposed that the P_M triplet is formed through a sequence of two spin-allowed excitations. In the first step, one of the pair of electrons in the HOMO of P_M is

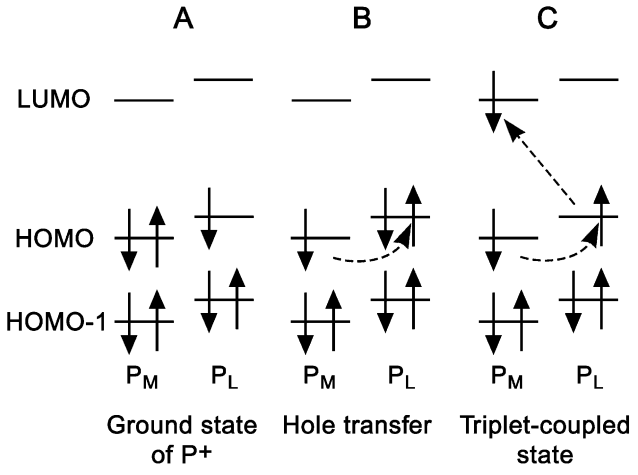

Fig. 9. Schematic of electronic transitions affecting P^+.

excited into the HOMO of P_L (hole transfer) (Fig. 9B). In the second step, the electron with opposite spin in the HOMO of P_L is excited into the lowest unoccupied molecular orbital (LUMO) of P_M, resulting in the formation of a triplet state with unpaired electrons with the same spin in both the HOMO and LUMO of P_M (Fig. 9C). This triplet state cannot be formed by direct excitation of an electron from the HOMO of P_M to LUMO of P_M because this would be spin-forbidden. The electronic configuration after this double excitation is referred to as a triplet-coupled state because it involves the participation of the partner BChl, P_L in the transition. As a result, this triplet-coupled state is dependent on the strength of the coupling between the two halves of the dimer [38,66].

Following from this, and ignoring for the moment additional modulating factors, it seems possible that there should be a correlation between the intensity of the P^+ band and the position of the P Q_y band, as both are dependent on the strength of the coupling between the P BChls. A decrease in the strength of this coupling should cause a decrease in the intensity of the P^+ absorbance band, and this should be accompanied by a blue-shift in the position of the P Q_y band. Fig. 10 shows that there is in fact a reasonable correlation between the absorbance maximum of the P Q_y band and the intensity of the P^+ band, in spectra of membrane-bound reaction centres at 30 K. This opens the possibility that the principal effect of this series of mutations is to decrease the strength of the coupling between the P_L and P_M BChls.

4.8. Indications from vibrational spectroscopy of a weakening of inter-dimer coupling

Further support for the proposal that the effects observed on the P Q_y and P^+ absorbance bands stem from a decrease in the coupling between the two halves of the P dimer comes from FTIR measurements of the absorbance band at 2600 cm^{-1} in the light-induced difference spectrum of the HL168F mutant [41]. This band has been attributed to a transition between the eigenstates ψ_a and ψ_b in the model of Parson et al. [43] described above. This transition is therefore directly related to the hole transfer from the HOMO of P_L to the HOMO of P_M that is the first step in the two step transition that forms the triplet-coupled state of P_M, and which gives rise to the P^+ band at 1245 nm (Fig. 9B). As with the P^+ band, the intensity of the electronic transition at 2600 cm^{-1} should be dependent on the strength of the coupling between the two halves of the dimer [38,66]. The intensity of this band is decreased by approximately 50% in the HL168F reaction centre (Fig. 5B).

Finally, as shown in Fig. 5A, there was also a decrease in the relative intensities of the bands at ~1290, 1480 and 1550 cm^{-1} in the light-induced FTIR difference spectrum of the HL168F mutant. These bands are characteristic of the dimeric P^+ cation, and are absent from the FTIR difference spectra of the heterodimer reaction centres [41,42], in which one of the dimer BChls is replaced by a BPhe and which therefore has a highly asymmetric primary donor. This similarity provides further evidence of a decrease in the strength of the coupling between the two halves of the P dimer in the HL168F mutant.

The conclusion from this analysis, therefore, is that changes in the absorbance properties of P and P^+ observed in this set of mutant complexes can be accounted for by postulating decreases in the strength of the inter-dimer coupling. This does not exclude the possibility that in some or all of these mutant complexes the position of the P Q_y band is also affected by other changes in the detailed structure of P and its environment, as discussed in the last section. Indeed additional modulation through changes in the conformation of the acetyl carbonyl group may account for some for the scatter in the plots in Fig. 10, including the behavior of the HL168F mutant.

4.9. Variations in the energy of the P^+ absorbance band

In addition to affecting the intensity of the P^+ absorbance band, the mutations also affected the absorbance

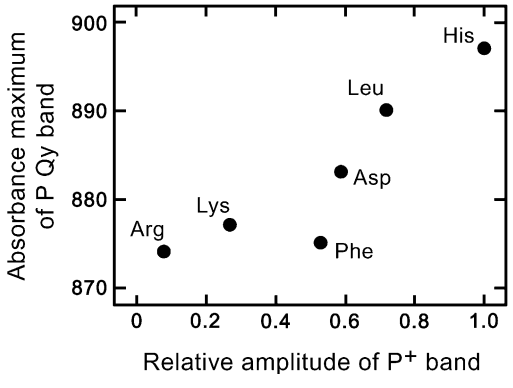

Fig. 10. Plot of the wavelength of maximum absorbance of the P Q_y band as a function of the relative amplitude of the P^+ band, in spectra of membrane-bound wild-type and mutant reaction centres recorded at 30 K.

maximum of this band. Such changes have been reported previously for reaction centres with mutations near the P BChls [19,61,67]. According to the interpretations of Reimers and Hush [38] and Reimers et al. [66], the wavelength of the absorbance band arising from the triplet-coupled transition (Fig. 9) corresponds to the energy gap between the HOMO and LUMO of P_M (i.e. it corresponds to the triplet absorption energy of the P_M BChl). In all of the mutant complexes with the exception of HL168F, the absorbance maximum of this band was shifted to longer wavelengths, implying a decrease in the size of this energy gap, whilst in the HL168F mutant this absorbance maximum exhibited a small blue-shift. These results indicate that, in addition to an unexpected effect on the energy of the HOMO of P_L due to breaking/weakening of the hydrogen bond donated by the L168 residue, the mutations at the L168 position also had some effect on the energy of the HOMO of the P_M BChl.

4.10. Electronic effects of the HL168F mutation

Another parameter that is known to be affected by the HL168F mutation is the electronic structure of the P^+ dimer. In single crystals of the wild-type reaction centre, ENDOR experiments on P^+ have shown that there is an unequal distribution of the π-spin density, with 68% of the positive charge located on the P_L BChl [68]. This asymmetry in the unpaired spin density has been accounted for by postulating molecular orbital models that contain an inequivalence in the Coulomb energies of the HOMOs of the P_M and P_L halves of the dimer [68,69]. Molecular orbital models of this sort have been used to investigate the optical and electronic properties of the primary donor [20,41,43,57,70–72].

In Fig. 11, we show such a model as it applies to the wild-type reaction centre, and illustrate possible effects of the HL168F mutation. Four orbitals are shown for each reaction centre, these being the HOMOs of the individual P_L and P_M BChls and two supermolecular orbitals. The HOMOs of the P_L and P_M BChls are inequivalent in energy by an amount $\Delta\alpha$, whilst the supermolecular orbitals are separated by an energy ΔE. The magnitude of ΔE is determined by $\Delta\alpha$ and the resonance integral, β_D, which is a measure of the strength of the interaction between the two BChls of the dimer. The energy required to remove an electron from P is denoted as E_m P/P$^+$. According to this model, the HOMO of the P_M BChl is located at a lower energy than that of the P_L BChl, with a result that most of the unpaired spin density in the P^+ state is located on the P_M half of the dimer. According to ENDOR spectroscopy, the P_L BChl is proposed to carry 68% of the positive charge of the cation radical [68].

In a series of papers, Lubitz, Allen and co-workers have shown that this model can be used to explain experimental data on the effects of introducing hydrogen bonds between the protein and the keto carbonyls of the P_L and P_M BChls [20,57,71,72]. Formation of a hydrogen bond to the P_M BChl through mutagenesis at the M160 position decreases

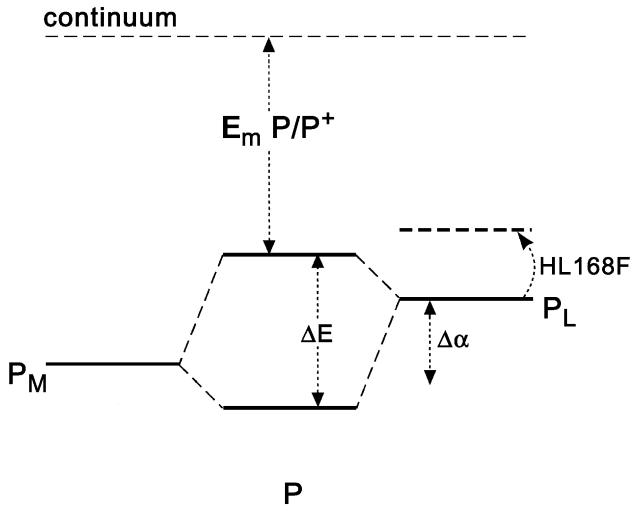

Fig. 11. Molecular orbital model for the primary donor BChl dimer, showing the interaction between the HOMOs of the P_L and P_M BChl. The monomer HOMOs are separated by the energy $\Delta\alpha$, and interact to produce two dimer orbitals that are separated by an energy ΔE. The HL168F mutation removes a hydrogen bond from the acetyl carbonyl of the P_L BChl, which is expected to destabilize the P_L half of the dimer. This will reduce the P/P$^+$ mid-point potential, E_m, and affect the distribution of unpaired spin density in P^+.

the energy of the HOMO of P_M, increasing E_m P/P$^+$ and making the distribution of unpaired spin density over the dimer more asymmetric. On the other hand, formation of a hydrogen bond to the P_L BChl through mutagenesis at the L131 position decreases the energy of the HOMO of P_L, increasing E_m P/P$^+$ but making the distribution of unpaired spin density more symmetric.

Taken together with values of E_m P/P$^+$, ENDOR data on the distribution of the unpaired spin density in P^+ shows that mutations that affect the acetyl carbonyl groups have more complex effects. The HL168F mutation removes the hydrogen bond between the protein and the acetyl carbonyl of P_L and this, in principle, should raise the energy of the HOMO of P_L (Fig. 11). In the absence of additional changes, this destabilization of the HOMO of P_L should have two effects. First, it should decrease E_m P/P$^+$, and this is in fact borne out by redox potentiometry that shows that P becomes easier to oxidize by 95 [15,17] or 115 mV (this work). The second expected effect of the mutation is to further increase the asymmetry of the spin density distribution in P^+ [20]. However, ENDOR experiments show that the HL168F mutation in fact causes a decrease in the percentage of the positive charge carried by P_L, from 68% in the wild-type reaction centre to 43% in the mutant [20].

In order to explain this discrepancy, and on the basis that in the 1PCR X-ray crystal structure of the wild-type reaction centre [3,4] the acetyl carbonyl of P_L is modeled as being significantly out-of-plane (see the discussion of this point in the Results), Rautter et al. [20] have postulated that the acetyl carbonyl of P_L undergoes a significant rotation to a more in-plane conformation in the HL168F mutant. It was

proposed that this rotation lowers the energy of the HOMO of P_L, counteracting the effect of removing the hydrogen bond [20]. A problem with this proposal is that, according to the model, this counteracting effect would also increase E_m P/P^+. In addition, this explanation is not supported by our crystallographic results which, in conjunction with structural data from our group and from others [21,25,45,47,73,74], argue against a marked out-of-plane geometry for the acetyl carbonyl of P_L in the wild-type reaction centre (see above). Furthermore, the structure of the HL168F mutant described in the present report demonstrates that the change in the conformation of this acetyl group is a 27° through-plane rotation, which would be equivalent to a small (~ 5°) net out-of-plane change in geometry. According to the arguments presented by Rautter et al. [20], this change would in fact further raise the energy of the HOMO of P_L, by slightly decreasing the strength with which the carbonyl group is conjugated to the π electron system of P.

On a related point, a feature of the primary donor is that hydrogen bonds donated by His residues to the acetyl carbonyl groups of the P_L and P_M BChls have a stronger effect on E_m P/P^+ (95/125 mV) than bonds donated by His residues to the keto carbonyls (60/80 mV) [19]. Ivancich et al. [57] have discussed a number of possible sources of this effect, including a significant reorientation of the acetyl group from a ~ 90° out-of-plane conformation to an in-plane conformation on mutating His L168 to Phe (and the reverse change on mutating the symmetry-related Phe M197 residue to His). As discussed above, the crystallographic data presented in this report do not agree with this interpretation.

In summary, therefore, our results argue against the proposal that, in the HL168F mutant, the decrease in the proportion of the positive charge of the cation radical carried by the P_L BChl is due to a large change in the orientation of the acetyl carbonyl of P_L, from an out-of-plane to in-plane conformation [20]. Presumably, one or more of the changes in the detailed structure of the P dimer that is consequent on the HL168F mutation produces the observed effect on the spin density distribution in P^+. One possible way to rationalize the experimental data with the molecular orbital model is to propose that the energy of the HOMO of the P_M BChl is also raised by the mutation. Raising the energies of the HOMOs of both BChls of the dimer could, in principle, create a situation where E_m P/P^+ is reduced and the P_L BChl carries only 42% of the charge of the cation radical. In support of this, the X-ray data we present for the HL168F mutant provide evidence that the detailed conformation of the P_M BChl is affected by the mutation (Fig. 8). However, to have the required effect, the HOMO of P_M would have to increase in energy by more than the HOMO of P_L, which is difficult to rationalize with the position of the mutated residue, and the relative effects of the mutation of the detailed conformations of P_L and P_M.

Finally, as pointed out by Lubitz, Artz et al. [71], another parameter in the molecular orbital model which may be very sensitive to mutations at the L168 position is the resonance integral, β_D. As described above, this parameter provides a measure of the strength of the interaction between the two BChls of the dimer. Plato et al. [70] have shown in studies of model dimers how variations in the ratio $\Delta\alpha/\beta_D$ produce considerable variations in the distribution of spin density over the dimer. However, in a scenario where the value of $\Delta\alpha$ is constant, a shift of the proportion of the charge of the cation carried by P_L from 68% to 42% would require an *increase* in β_D. This conclusion is clearly in disagreement with the interpretation of the optical effects of the HL168F mutation, that there is in fact a decrease in the strength of this coupling.

4.11. Changes in the protein–cofactor structure on mutation of His L168

Fig. 8 summarises the changes in the structure of the P BChls that result from the replacement of His L168 by Phe. As there was no flexing of the polypeptide backbone, the bulkier Phe residue made a closer approach to ring I and the acetyl carbonyl group of the P_L BChl, pushing this part of the macrocycle towards that of the P_M BChl and pushing the acetyl carbonyl group below the plane of the macrocycle. This movement was small (maximally 0.5 Å) but distinct, and included a component that was parallel to the plane of the P_L macrocycle.

The most obvious consequence of this movement of the P_L BChl was to decrease the separation between the two BChls of the P dimer, by between 0.1 and 0.3 Å. On the basis of many computational studies (e.g. see Ref. [63]), such a change would be expected to increase the coupling between the P_L and P_M BChl, and produce a red-shift of the P Q_y band. In fact, as described above, the P Q_y band is blue-shifted in the HL168F mutant, and other spectroscopic information provides strong indications that there is a decrease in inter-dimer coupling in this complex. At this point, it is also worth noting that essentially the same change in dimer structure has been seen in a HL168F mutant of the *Rps. viridis* reaction centre, where again the P Q_y band exhibits a significant blue-shift. Presumably, if the decrease in inter-dimer spacing seen in the HL168F reaction centre does produce an increase in inter-dimer coupling, this must be (over)-compensated for by other changes in the structure of the protein that decrease the strength of the inter-dimer coupling.

It seems unlikely that the changes in structure of the P BChls observed in the HL168F mutant will also be present in all of the remaining mutants, as these changes seem to be due to the steric problems created by replacing a His residue with a more bulky Phe residue. In the case of the HL168L and HL168D mutants, for example, Leu and Asp are of a similar size to His (van der Waals volumes of 124 and 91 $Å^3$ for the Leu and Asp residue, respectively, compared with 118 $Å^3$ for His [75]). Modeling studies indicate that either Leu or Asp could be substituted for His without creating the steric problems seen in the HL168F mutant (data not

shown), and cause relatively little disturbance to the structure of the surrounding protein–cofactor matrix. This may be why these two mutations have the smallest effect on inter-dimer coupling, as assessed by the position of the P Q_y band and intensity of the P^+ band (Fig. 10).

Both Arg and Lys are larger residues than His (148 and 135 $Å^3$, respectively [75]) and have an elongated shape. Modeling studies indicate that these residues will not fit into the cavity created by the removal of His L168 without some disturbance to the structure of the surrounding protein–cofactor matrix, or a significant change in the gross orientation of the Arg or Lys residue. As an illustration of the latter, an X-ray crystal structure has been published for a reaction centre with a Phe to Arg mutation at the symmetry-related M197 position [25,58]. In that study, the Arg residue was found to have adopted a conformation that was quite distinct from that adopted by the wild-type Phe residue, occupying a cleft at the interface of the L- and M-subunits and interacting with residue Asp L155 at the periplasmic surface of the protein. This reorientation created a cavity that was occupied by at least two water molecules [58]. As discussed in detail previously [25], the symmetry-related His L168 is also "visible" from the periplasmic surface of the protein via a cleft at the interface of the L- and M-subunits, and the symmetry-related residue to Asp L155 is also an acidic amino acid (Asp M184). However, the cleft adjacent to the L168 residue is much narrower than that near the M197 residue [25]. It is therefore possible that an Arg or Lys residue at the L168 position may have undergone a gross change in orientation, along the lines seen in X-ray structure of the Arg M197 mutant, although this would probably cause some additional changes in the packing of amino acids in the immediate vicinity of Arg L168 [25].

5. Summary

The spectroscopic analysis presented in this report indicates that the general effect of replacement of His L168 with either an acidic, basic or nonpolar residue is to decrease in the strength of the electronic coupling between the two halves of the P dimer. This produces a correlated decrease in the intensity of the P^+ absorbance band and a blue-shift of the P Q_y band. There is also a decrease in the intensity of bands in the FTIR spectrum of the HL168F mutant that are characteristic of a dimeric primary donor, including the inter-dimer transition at 2600 cm^{-1}. It seems likely that the precise nature of the changes in protein–cofactor structure that brings about this decrease in coupling will be different in each of the mutants. In the particular case of the HL168F mutant, the effect on the inter-dimer coupling has to be rationalized with the counter-intuitive observation that the inter-dimer spacing is slightly decreased. Subtle changes in the separation of the P and B_A BChls may explain why this mutation has little effect on the rate of primary electron transfer in the *Rb. sphaeroides* reaction centre, but brings about a dramatic acceleration of primary electron transfer in the *Rps. viridis* complex.

Acknowledgements

This work was supported by the Biotechnology and Biological Sciences Research Council of the United Kingdom, the Human Capital and Mobility Programme and Wellcome Trust grant 043492.

References

[1] J.P. Allen, G. Feher, T.O. Yeates, H. Komiya, H.D.C. Rees, Proc. Natl. Acad. Sci. U. S. A. 84 (1987) 5730–5734.
[2] C.-H. Chang, O. El-Kabbani, D. Tiede, J. Norris, M. Schiffer, Biochemistry 30 (1991) 5352–5360.
[3] U. Ermler, G. Fritzsch, S.K. Buchanan, H. Michel, Structure 2 (1994) 925–936.
[4] U. Ermler, H. Michel, M. Schiffer, J. Bioenerg. Biomembranes 26 (1994) 5–15.
[5] W.W. Parson, in: H. Scheer (Ed.), Chlorophylls, CRC Press, Boca Raton, FL, USA, 1991, pp. 1153–1180.
[6] G.R. Fleming, R. Van Grondelle, Phys. Today 47 (1994) 48–55.
[7] N.W. Woodbury, J.P. Allen, in: R.E. Blankenship, M.T. Madigan, C. Bauer (Eds.), Anoxygenic Photosynthetic Bacteria, Kluwer, The Netherlands, 1995, pp. 527–557.
[8] W.W. Parson, in: D.S. Bendall (Ed.), Protein Electron Transfer, BIOS Scientific Publishers, Oxford, 1996, pp. 125–160.
[9] A.J. Hoff, J. Deisenhofer, Phys. Rep. 287 (1997) 1–247.
[10] M.E. van Brederode, M.R. Jones, in: N.S. Scrutton, A. Holtzenburg, (Eds.), Enzyme-Catalysed Electron and Radical Transfer, Kluwer Academic/Plenum Publishers, New York, USA, 2000, pp. 621–676.
[11] K.L. Hanson, in: H. Scheer (Ed.), Chlorophylls, CRC Press, Boca Raton, FL, USA, 1991, pp. 993–1014.
[12] K.V.P. Nagashima, K. Matsuura, N. Wakao, A. Hiraishi, K. Shimada, Plant Cell Physiol. 38 (1997) 1249–1258.
[13] E. Nabedryk, J. Breton, J.P. Allen, H.A. Murchison, A.K.W. Taguchi, J.C. Williams, N.W. Woodbury, in: J. Breton, A. Vermeglio (Eds.), The Photosynthetic Bacterial Reaction Centre II: Structure, Spectroscopy and Dynamics, Plenum, New York, 1992, pp. 141–145.
[14] H.A. Murchison, R.A. Alden, J.P. Allen, J.M. Peloquin, A.K.W. Taguchi, N.W. Woodbury, J.C. Williams, Biochemistry 32 (1993) 3498–3505.
[15] X. Lin, J.C. Williams, J.P. Allen, P. Mathis, Biochemistry 33 (1994) 13517–13523.
[16] X. Lin, H.A. Murchison, V. Nagarajan, W.W. Parson, J.P. Allen, J.C. Williams, Proc. Natl. Acad. Sci. U. S. A. 91 (1994) 10265–10269.
[17] T.A. Mattioli, J.C. Williams, J.P. Allen, B. Robert, Biochemistry 33 (1994) 1636–1643.
[18] J.P. Allen, J.C. Williams, J. Bioenerg. Biomembranes 27 (1995) 275–283.
[19] T.A. Mattioli, X. Lin, J.P. Allen, J.C. Williams, Biochemistry 34 (1995) 6142–6152.
[20] J. Rautter, F. Lendzian, C. Schulz, A. Fetsch, M. Kuhn, X. Lin, J.C. Williams, J.P. Allen, W. Lubitz, Biochemistry 34 (1995) 8130–8134.
[21] C.R.D. Lancaster, M.V. Bibikova, P. Sabatino, D. Oesterhelt, H. Michel, J. Biol. Chem. 275 (2000) 39364–39368.
[22] C. Rischel, D. Spiedel, J.P. Ridge, M.R. Jones, J. Breton, J.C. Lambry, J.L. Martin, M.H. Vos, Proc. Natl. Acad. Sci. U. S. A. 95 (1998) 12306–12311.
[23] M.R. Jones, M. Heer-Dawson, T.A. Mattioli, C.N. Hunter, B. Robert, FEBS Lett. 339 (1994) 18–24.

[24] J.E. O'Reilly, Biochim. Biophys. Acta 292 (1973) 509–515.
[25] K.E. McAuley-Hecht, P.K. Fyfe, J.P. Ridge, S.M. Prince, C.N. Hunter, N.W. Isaacs, R.J. Cogdell, M.R. Jones, Biochemistry 37 (1998) 4740–4750.
[26] K.E. McAuley, P.K. Fyfe, J.P. Ridge, N.W. Isaacs, R.J. Cogdell, M.R. Jones, Proc. Natl. Acad. Sci. U. S. A. 96 (1999) 14706–14711.
[27] Z. Otwinowski, W. Minor, Methods Enzymol. 276 (1997) 307–326.
[28] J. Navaza, Acta Crystallogr., A 50 (1994) 157–163.
[29] G.N. Murshudov, A.A. Vagin, E.J. Dodson, Acta Crystallogr., D Biol. Crystallogr. 53 (1997) 240–253.
[30] M.D. Winn, M.N. Isupov, G.N. Murshudov, Acta Crystallogr., D Biol. Crystallogr. 57 (2000) 122–133.
[31] P.J. Kraulis, J. Appl. Crystallogr. 24 (1991) 946–950.
[32] E.A. Merrit, D.J. Bacon, Methods Enzymol. 277 (1997) 505–524.
[33] D.E. McRee, J. Mol. Graph. 10 (1992) 44–46.
[34] M.R. Jones, G.J.S. Fowler, L.C.D. Gibson, G.G. Grief, J.D. Olsen, W. Crielaard, C.N. Hunter, Mol. Microbiol. 6 (1992) 1173–1184.
[35] M.R. Jones, R.W. Visschers, R. van Grondelle, C.N. Hunter, Biochemistry 31 (1992) 4458–4465.
[36] V.A. Shuvalov, W.W. Parson, Proc. Natl. Acad. Sci. U. S. A. 78 (1981) 957–961.
[37] A. Verméglio, G. Paillotin, Biochim. Biophys. Acta 681 (1982) 32–40.
[38] J.R. Reimers, N.S. Hush, J. Am. Chem. Soc. 117 (1995) 1302–1308.
[39] E. Nabedryk, J.P. Allen, A.K.W. Taguchi, J.C. Williams, N.W. Woodbury, J. Breton, Biochemistry 32 (1993) 13879–13885.
[40] E. Nabedryk, C. Schulz, F. Müh, W. Lubitz, J. Breton, Photochem. Photobiol. 71 (2000) 582–588.
[41] J. Breton, E. Nabedryk, W.W. Parson, Biochemistry 31 (1992) 7503–7510.
[42] E. Nabedryk, S.J. Robles, E. Goldman, D.C. Youvan, J. Breton, Biochemistry 31 (1992) 10852–10858.
[43] W.W. Parson, E. Nabedryk, J. Breton, in: J. Breton, A. Vermeglio (Eds.), The Photosynthetic Bacterial Reaction Centre II: Structure, Spectroscopy and Dynamics, Plenum, New York, (1992) 79–88.
[44] W. Kabsch, Acta Crystallogr., A 32 (1976) 922–923.
[45] K.E. McAuley, P.K. Fyfe, J.P. Ridge, R.J. Cogdell, N.W. Isaacs, M.R. Jones, Biochemistry 39 (2000) 15032–15043.
[46] J.P. Ridge, M.E. van Brederode, M.G. Goodwin, R. van Grondelle, M.R. Jones, Photosynth. Res. 59 (1999) 9–26.
[47] K.E. McAuley, P.K. Fyfe, R.J. Cogdell, N.W. Isaacs, M.R. Jones, FEBS Lett. 467 (2000) 285–290.
[48] M.R. Jones, P.K. Fyfe, A.W. Roszak, N.W. Isaacs, R.J. Cogdell, Biochim. Biophys. Acta, in press.
[49] M.H. Vos, J.L. Martin, Biochim. Biophys. Acta 1411 (1999) 1–20.
[50] M.H. Vos, C. Rischel, M.R. Jones, J.-L. Martin, Biochemistry 39 (2000) 8353–8361.
[51] C. Rischel, D. Spiedel, J.P. Ridge, M.R. Jones, J. Breton, J.C. Lambry, J.L. Martin, M.H. Vos, Proc. Natl. Acad. Sci. U. S. A. 95 (1998) 12306–12311.
[52] K. Czarnecki, J.R. Diers, V. Chynwat, J.P. Erickson, H.A. Frank, D.F. Bocian, J. Am. Chem. Soc. 119 (1997) 415–426.
[53] T. Arlt, M. Bibikova, H. Penzkofer, D. Oesterhelt, W. Zinth, J. Phys. Chem. 100 (1996) 12060–12065.
[54] C.R.D. Lancaster, M.V. Bibikova, P. Sabatino, D. Oesterhelt, H. Michel, J. Biol. Chem. 275 (2000) 39364–39368.
[55] H. Michel, O. Epp, J. Deisenhofer, EMBO J. 5 (1986) 2445–2451.
[56] T.O. Yeates, H. Komiya, A. Chirino, D.C. Rees, J.P. Allen, G. Feher, Proc. Natl. Acad. Sci. U. S. A. 85 1988, pp. 7993–7997.
[57] A. Ivancich, K. Artz, J.C. Williams, J.P. Allen, T.A. Mattioli, Biochemistry 37 (1998) 11812–11820.
[58] J.P. Ridge, P.K. Fyfe, K.E. McAuley, M.E. van Brederode, B. Robert, R. van Grondelle, N.W. Isaacs, R.J. Cogdell, M.R. Jones, Biochem. J. 351 (2000) 567–578.
[59] Y. Jia, T.J. DiMagno, C.-K. Chan, Z. Wang, M. Du, D.K. Hanson, M. Schiffer, J.R. Norris, G.R. Fleming, J. Phys. Chem. 97 (1993) 13180–13191.
[60] V. Nagarajan, W.W. Parson, D. Davis, C.C. Schenck, Biochemistry 32 (1993) 12324–12336.
[61] J. Wachtveitl, J.W. Farchaus, P. Mathis, D. Oesterhelt, Biochemistry 32 (1993) 10894–10904.
[62] L.M.P. Beekman, I.H.M. van Stokkum, R. Monshouwer, A.J. Rijnders, P. McGlynn, R.W. Visschers, M.R. Jones, R. van Grondelle, J. Phys. Chem. 100 (1996) 7256–7268.
[63] M.A. Thompson, M.C. Zerner, J. Fajer, J. Phys. Chem. 95 (1991) 5693–5700.
[64] W.W. Parson, A. Warshel, J. Am. Chem. Soc. 109 (1987) 6152–6163.
[65] E. Gudowska-Nowak, M.D. Newton, J. Fajer, J. Phys. Chem. 94 (1990) 5795–5801.
[66] J.R. Reimers, M.C. Hutter, N.S. Hush, Photosynth. Res. 55 (1998) 163–171.
[67] J.C. Williams, R.G. Alden, H.A. Murchison, J.M. Peloquin, N.W. Woodbury, J.P. Allen, Biochemistry 31 (1992) 11029–11037.
[68] F. Lendzian, M. Huber, R.A. Isaacson, B. Endeward, M. Plato, B. Boenigk, K. Möbius, W. Lubitz, G. Feher, Biochim. Biophys. Acta 1183 (1993) 139–160.
[69] J. Rautter, F. Lendzian, W. Lubitz, S. Wang, J.P. Allen, Biochemistry 33 (1994) 12077–12084.
[70] M. Plato, F. Lendzian, W. Lubitz, K. Möbius, in: J. Breton, A. Vermeglio (Eds.), The Photosynthetic Bacterial Reaction Centre II: Structure, Spectroscopy and Dynamics, Plenum, New York, 1992, pp. 109–118.
[71] K. Artz, J.C. Williams, J.P. Allen, F. Lendzian, J. Rautter, W. Lubitz, Proc. Natl. Acad. Sci. U. S. A. 94 (1997) 13582–13587.
[72] F. Müh, J. Rautter, W. Lubitz, Biochemistry 36 (1997) 4155–4162.
[73] M.H.B. Stowell, T.M. McPhillips, D.C. Rees, S.M. Soltis, E. Abresch, G. Feher, Science 276 (1997) 812–816.
[74] H.L. Axelrod, E.C. Abresch, M.L. Paddock, M.Y. Okamura, G. Feher, Proc. Natl. Acad. Sci. U. S. A. 97 (2000) 1542–1547.
[75] T.E. Creighton, Proteins, 2nd edn., Freeman, New York, 1993, p. 4.
[76] A.T. Brünger, Nature 335 (1992) 472–475.
[77] R.W.W. Hooft, G. Vriend, C. Sander, E.E. Abola, Nature 381 (1996) 272.
[78] R.A. Laskowski, W.W. MacArthur, D.S. Moss, J.M. Thornton, J. Appl. Crystallogr. 26 (1993) 283–291.
[79] D.W.J. Cruickshank, Acta Crystallogr., D Biol. Crystallogr. 55 (1999) 583–601.